**Acknowledgements**

I'd like to thank my advisor Dr. Vicki L. Hansen for being the most enthusiastic and knowledgeable geologist that I have had the pleasure of working with and Dr. Scott Freundschund and Dr. John Goodge for being a part of my committee and helping me with the GIS and petrography aspects of my thesis. I'd also like to thank the University of Minnesota Duluth, the UMD College of Science and Engineering, the UMD Department of Geology, the University of Minnesota Twin Cities, the Precambrian Research Center, the National Resources Research Institute, the Geological Society of America, the UM grant-in-aid granted to J. Goodge and the Institute on Lake Superior Geology for field, laboratory and travel support. My thanks also extend to the McKnight Foundation for summer housing funds granted to V. L. Hansen through the McKnight Presidential Endowment. I had the opportunity to be a fellow for a NSF funded grant through the UMD Mathematics and Statistics Department and would like to give thanks for tuition support granted through my second year of graduate school. I must mention my fellow Shear Zone Ladies, Sally Goodman, Susie Karberg and Jenny Koester for all their helpful comments and advice. Thanks also goes to my field assistant Hillary McGown for bushwhacking through the woods and rowing in the canoe with me! Finally, thank you for your encouragement, patience and support to everyone back in Washington and Oregon who missed me while I was earning my MS degree in Duluth, Minnesota!

**Abstract**

The debate about the formation of Archean (3.8-2.5 Ga) granite-greenstone terrains feature two hypotheses: 1) sagduction and diapirism and 2) arc-terrane accretion via plate tectonics processes. The Superior Province in northeastern Minnesota is an Archean granite-greenstone terrain which is historically explained by arc-terrane accretion.

This work involves a structural and kinematic analysis of the deformational processes within the Shagawa Lake shear zone, northeastern Minnesota. The Shagawa Lake shear zone, a zone of L-S tectonites that, strikes east-northeast and dips steeply, to lies within a greenstone belt bordered to the north and south by granitic complexes. This work focuses on an ~18 km long and ~3-4 km wide portion of the shear zone. Structural data were collected and compiled and oriented samples were collected for microstructural analysis.

The Shagawa Lake shear zone foliation averages 065, 80 S. Elongation lineation (Le) defines two major populations, a moderately to steeply-plunging group (90 ±30) and a shallowly-plunging group (15 ±10). Strike-slip Le are few and overprint the pervasive dip-slip Le.

Shear sense was interpreted in 34 thin sections within the L-S tectonite motion plane, normal to foliation and parallel to Le. Microstructural kinematic data indicate that both south-side-up and north-side-up displacement occurred along and across the shear zone; no discernable spatial pattern emerged within the shear domains. L-S tectonites with east-plunging Le indicate either south- or north-side-up shear parallel to Le, whereas

L-S tectonites with west-plunging Le dominantly indicate north-side-up shear parallel to Le. Strike-slip L-S tectonites record sinistral shear.

Overprinting relationships and the kinematic patterns within the Shagawa Lake shear zone are consistent with the relative rise of the southern region followed by rise of the northern region. Within the Vermilion District the Giants Range Batholith (south) and Vermilion Granitic Complex (north) may represent the rising southern and northern regions respectively, with the volcanic basin concurrently sinking.

**Table of Contents**

**Tables**

**List of Figures**

**List of Plates**

## 1. Introduction

Granite-greenstone terrains are a dominant and consistent feature found only within Archean (3.8-2.5 Ga) cratons. The process of Archean granite-greenstone terrains formation is widely disputed, and two opposing hypotheses persist: (1) sagduction and diapirism caused by crustal-scale density instabilities that led to sinking of greenstone basins and rise of granitic bodies (McGregor, 1951; Anhauesser et al., 1969; Mareschal and West, 1980; Collins et al., 1998; Chardon et al., 2002; Rey et al., 2003; Van Kranendonk, 2004), and (2) modern-style arc-terrane accretion via plate tectonics processes which led to interlayered volcanic basins and volcanic-arc plutons (Windley, 1984; Card, 1990; Stanley, 1992; Kimura et al., 1993; Cawood, 2006). Diapirism was originally the favored hypothesis for the formation of Archean granite-greenstone terrains but with the formulation and acceptance of modern plate tectonics theory, post 1970's research has focused on the arc-terrane accretion hypothesis, especially within the Superior Province of North America.

The Superior Province in northeastern Minnesota is an Archean granite-greenstone terrain (Fig. 1) which has been historically attributed to arc-terrane accretion (e.g., Bauer and Bidwell, 1990; Card, 1990; Czech and Hudleston, 2003), yet no robust evidence or arguments have been put forth to disprove the sagduction/diapirism hypothesis. Many structural features within the granite-greenstone terrains are not predicted by the arc-terrane accretion hypothesis, such as moderately to steeply-plunging elongation lineations (Le) (will justify Le later) and diffuse shear zones (Lin,

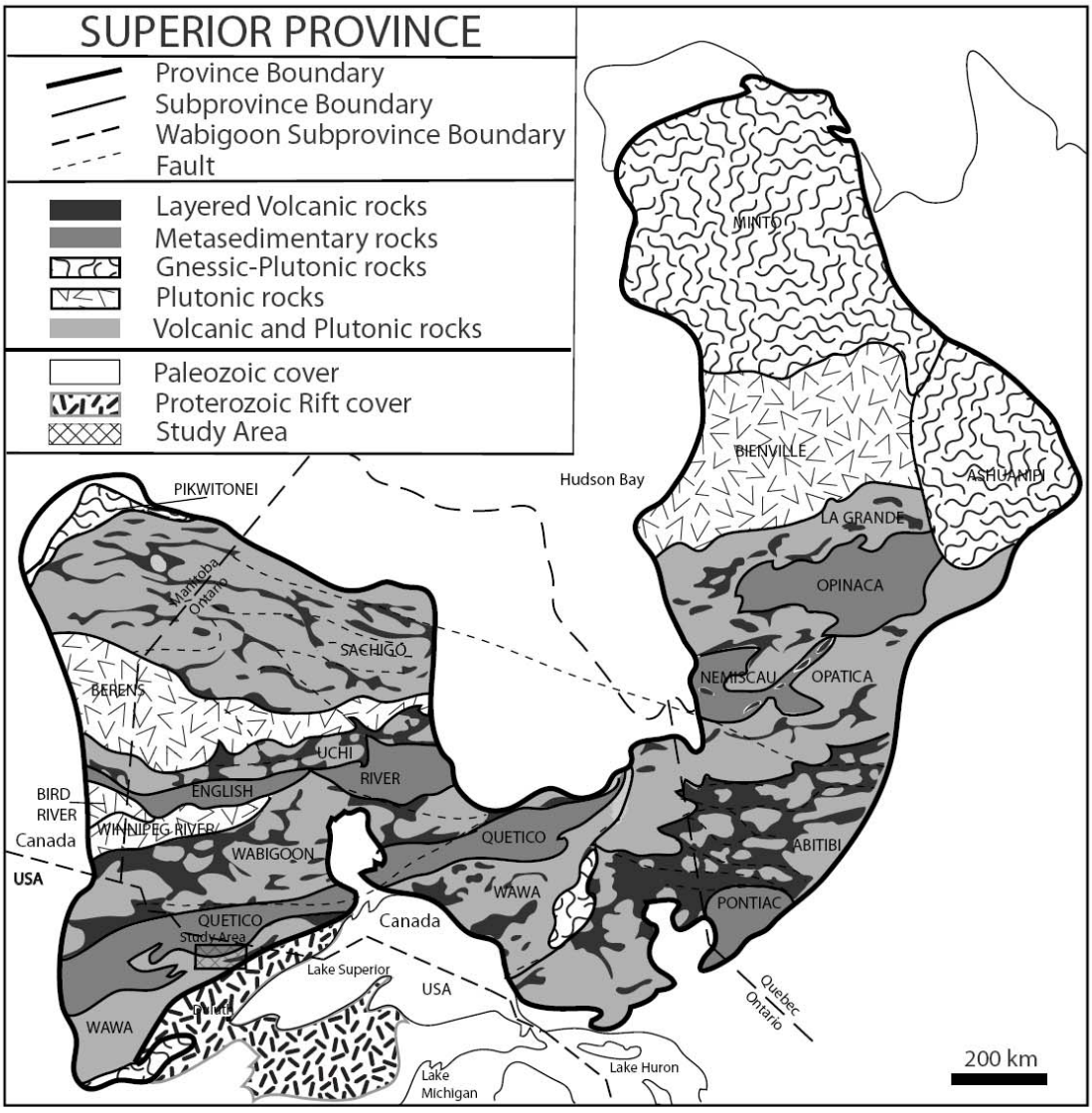


Figure 1. Map of the Superior Province showing simplified subprovinces and location of study area. Simplified from Card (1990). Box indicating study area in Figure 4.

2005), which might be more easily reconciled with sagduction/diapirism processes. It is unclear which hypothesis most adequately explains the structural evolution of the Archean granite-greenstone terrains within northeastern Minnesota.

The east-northeast striking, steeply-dipping Shagawa Lake shear zone in northeastern Minnesota lies within an Archean greenstone belt bordered to the north by the Vermilion Granitic Complex and to the south by the Giants Range Batholith. Shear zones within greenstone terrains can provide critical insight into Archean geologic processes, because they are the locus of displacement involved in development of granite-greenstone terrains.

I performed an analysis of the Shagawa Lake shear zone to determine the structural and kinematic history as an example of a representative Archean granite-greenstone terrain in northeastern Minnesota. Field and laboratory work included measuring foliation and Le, and analysis of oriented thin sections for microstructural indicators.

This paper highlights structural and kinematic relationships within the Shagawa Lake shear zone shown by foliation, Le orientations, and microstructural kinematic interpretations. Foliation trajectories are generally straight along the strike of the shear zone and Le orientations are mostly steep with regions of shallow and oblique plunging Le that exhibit no clear spatial pattern. Based on microstructural data, shear sense is recorded in the plane perpendicular to foliation and parallel to Le. Kinematic indicators record both south-side-up and north-side-up shear with no apparent pattern along and across the shear zone. East-plunging Le dominantly indicates south-side-up shear and west-plunging Le consistently indicates north-side-up shear. Locally, north-side-up shear

overprints dominantly south-side-up shear in two thin sections from adjacent field locations. Strike-slip shear occurs in a localized zone that might overprint the early oblique to dip-slip shear. Two samples record sinistral strike-slip shear. Structural data neither prove nor disprove either hypothesis because the foliation and Le are widely distributed in orientation and location.

Structural data do not exhibit an ideal pattern of either hypothesis. Kinematic patterns within the shear zone, however, are consistent with rising of the southern and northern granitic complexes and concurrent sinking of greenstone basins, forming south-side-up and north-side-up oblique- to dip-slip shear within the greenstones and volcanic sediments. Within the Shagawa Lake shear zone, relative displacement with respect to bounding granite bodies indicates that the southern Giants Range Batholith rose early, followed by rise of the northern Vermilion Granitic Complex. Late dextral displacement along the Vermilion Fault can account for laterally displaced rock units on published geologic maps.

## 2. Archean Cratons

Debate about the formation of granite-greenstone terrains within Archean cratons continues. The two prevailing hypotheses will be explained broadly in the context of granite-greenstone terrains around the world and then I will focus on the Superior Province in northeastern Minnesota.

### 2.1 Granite-Greenstone Terrains: Sagduction/Diapirism versus Arc-terrane Accretion

Archean granite-greenstone terrains define basin-shaped narrow linear belts of metamorphosed volcanic rocks that surround round to elliptical shaped granitic complexes (Anhauesser et al., 1969). The first substantial research of granite-greenstone terrains was performed in the Rhodesia Craton in South Africa. The greenstone units rapidly thin away from the center of thick basins and consistently trend around the distinct elliptical to round-shaped granite bodies (Anhauesser et al., 1969; McGregor, 1951). The elliptical shape of the granites and surrounding elongate greenstone belts in all Archean granite-greenstone terrains was some of the first evidence used to formulate the sagduction/diapirism hypothesis.

The sagduction/diapirism hypothesis involves two steps starting with Earth's originally differentiated crust marked by variations in crustal thickness: 1) volcanism from the mantle and deposition of volcanic packages within thin regions of the crust, and 2) density instabilities that cause volcanic packages to sink into basins and granitoids to rise to the surface (Fig. 2) (Anhaeusser, 1969; Rey et al., 2003; Van Kranendonk, 2004).

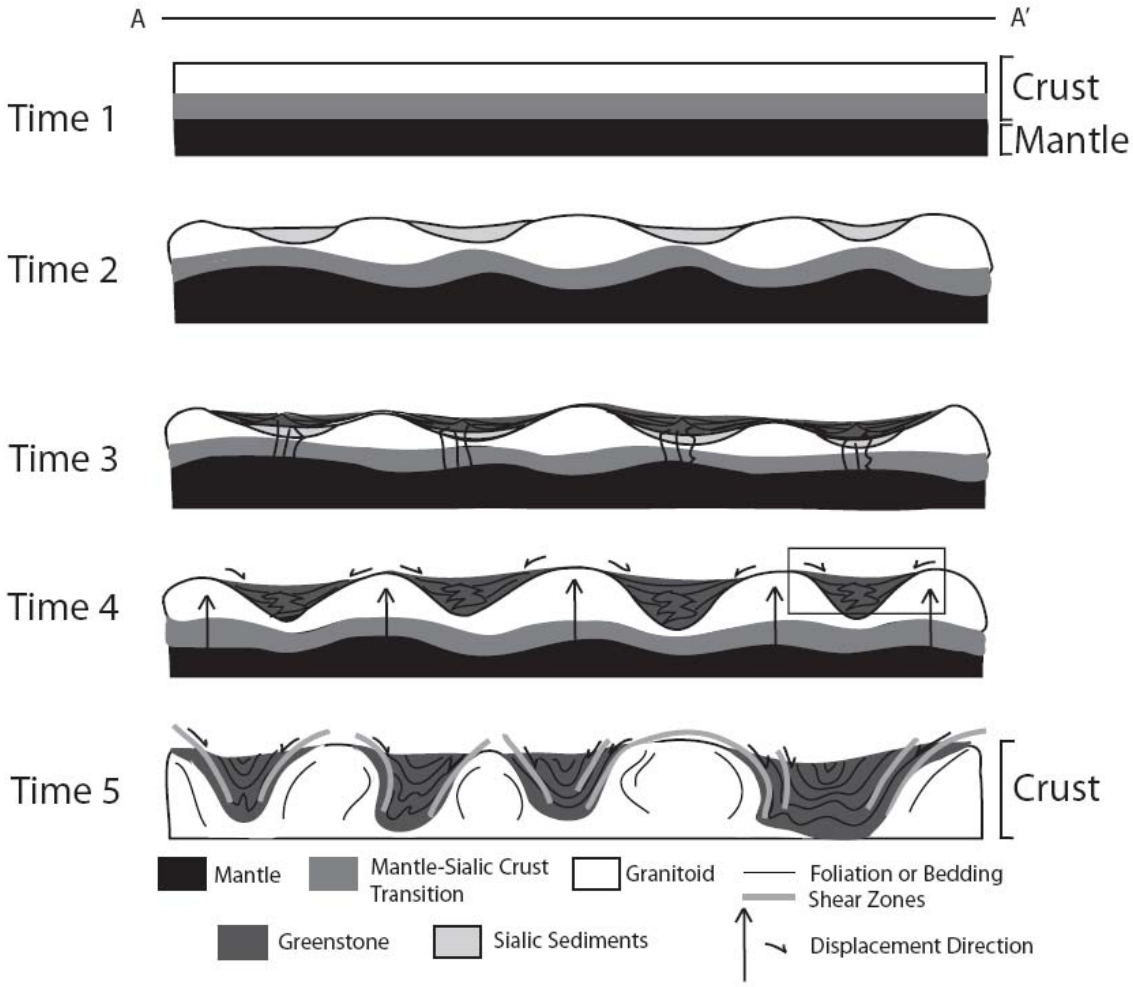


Figure 2. Cartoon of sagduction/diapirism. Time 1 = original differentiation of Earth's sialic crust. Time 2 = erosion and deposition of sediments from sialic crust. Time 3 = volcanism from the mantle in thin areas of the crust. Time 4 = initiation of density driven sagging of volcanic-sedimentary basins and diapiric rise of granitoids. Time 5 = conclusion of density reorganization of the upper crust, final stage of crustal assembly. Line A to A' is representative of a north-south cross section on Fig 1. Box in Time 4 refers to Figure 5. (Modeled after Rey et al., 2003; Anhauesser, 1969; and Van Kranendonk et al., 2001).

The sagduction/diapirism hypothesis predicts: 1) narrow basins of volcanic rocks between adjacent granite bodies, 2) steeply-dipping metamorphic foliation and steeply-plunging Le within greenstone belts, 3) structural transition from steep (basin center) to shallow towards the edge of the granite bodies, and 4) a transition from low- to moderate-T metamorphic facies towards the granite bodies within the greenstone belts (Collins et al., 1998; Chardon et al., 2002; Hickman, 2003: Rey et al., 2003; Van Kranendonk, 2004, Sandiford, 2004). A high geothermal gradient during the Archean may have facilitated the sagduction/diapirism process. Gravitational forces would have had a greater effect in the Archean due to weaker crust and could have assisted the concomitant sagging of greenstone belts and diapiric rise of granitoids (Rey and Houseman, 2006).

The arc-terrane accretion hypothesis involves convergence of island arcs upon continental crust by means of modern-style plate tectonic processes (Windley, 1984; Chadwick et al., 2000; Card, 1990; Cawood, 2006; Krapez and Barley, 2008) (Fig. 3). The arc-terrane accretion hypothesis predicts that: 1) Archean lithosphere was strong and was capable of sustaining convergence, 2) foliations formed parallel to the subduction margin, 3) the upper-plate age provinces young toward the subducting plate margin, and 4) crustal domains include evidence for volcanic arcs, fore-arcs and back-arc basins (Card, 1990).

Various structural, geochemical and stratigraphic studies of granite-greenstone terrains in Archean cratons of South Africa, Australia, India and Greenland do not conclusively support sagduction/diapirism over arc-terrane accretion or vice-versa.

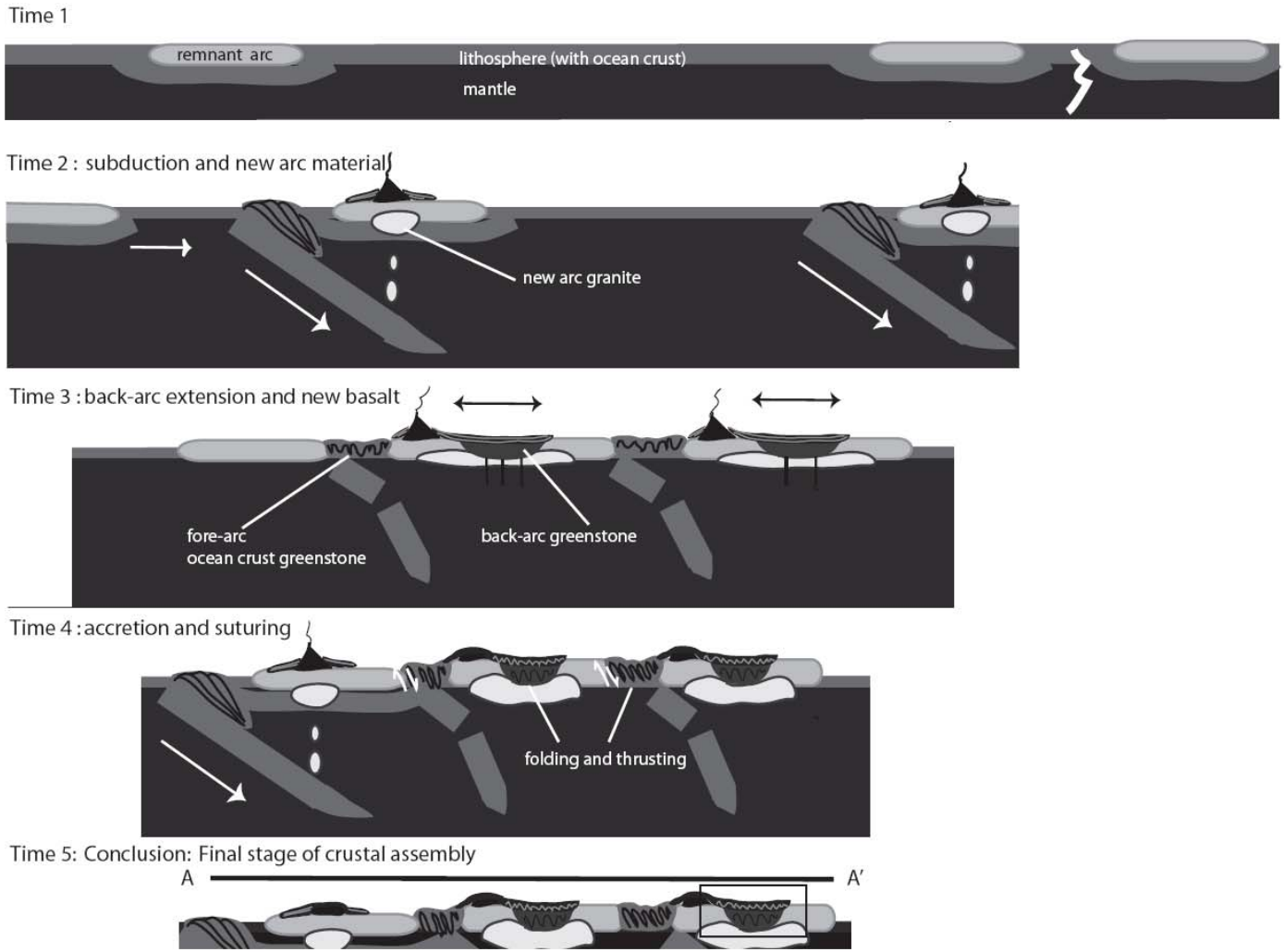


Figure 3. Cartoon of granite-greenstone terrain formation by arc-terrane accretion. This figure shows both back-arc and fore-arc greenstone formation. Line A to A' is representative of a north-south cross section of figure 1. The box in time step 5 refers to figure 4 cross section (Modified after Windley, 1977; Stanley, 1992; Kimura et al., 1993).

In some granite-greenstone terrains, a variable Le displays steep to shallow plunge along the edge of granite bodies. These relations are attributed to the initiation of density instabilities with the greenstones shedding off rising granites, thereby mimicking the granite shape (Collins et al., 1998; Chardon et al., 2002; Rey et al., 2003; Van Kranendonk et al., 2004). In the Bindura-Shamva greenstone belt in Zimbabwe displacement between adjacent batholiths caused obliquely plunging Le. Conversely, synorogenic basins in the Western Australian Yilgarn craton are similar to modern arc-terrane accretion settings by displaying linear zones of subsidence adjacent to zones of strike-slip displacement (Krapez and Barley, 2008). In Greenland's Isua Greenstone Belt (~3.64 Ga), based on structural studies Hanmar and Greene (2002) concluded that the scale and style of crustal deformation is similar to modern thrust-nappe stacking, implying that plate tectonic processes were operative.

Geochemical data are also invoked to explain the origin of granite-greenstone terrains and more specifically the granite bodies. The granite to greenstone ratio within granite-greenstone terrains is 4:1 spurring the question "Where did the large amounts of granite come from?" Trace element geochemical data are interpreted as evidence that granites formed from reworked sialic crustal material (Anhaeusser, 1969; Condie et al., 1982), consistent with either hypothesis. Granites can be emplaced both during and directly after sagduction/diapirism readily explaining the syn- and post-deformation granites that exist in granite-greenstone terrains (Arth and Hanson, 1975). However, Engle (1968) argued that K, U, Th, and Pb trace element values of the Archean Rhodesia craton in South Africa are similar to Phanerozoic crust, which he interprets as evidence that lithosphere forming processes were similar in the Archean and the Phanerozoic. On

this basis he argues for a plate tectonics related origin of granite-greenstone terrains. The origin of granites in granite-greenstone terrains remains unclear.

Stratigraphic data have been proposed to support both hypotheses. The stratigraphic location of greenstone terrains around dome-shaped granitic bodies is consistent with the sagduction/diapirism hypothesis. Stratigraphic data in favor of arc-terrane accretion suggest sediment was deposited in back-arc settings where extension was steady and directly related to tectonic convergence and uplift (Krapez and Barley, 2008).

The Archean lithospheric geothermal gradient was likely higher than today, and is an important factor to consider when studying Archean granite-greenstone terrains. The Archean crust was characterized by3-4 times greater heat production from radioactive isotope decay and a higher geothermal gradient due to greater heat production and a strong greenhouse effect from high concentrations of carbon dioxide ($CO_2$) and methane ($CH_4$) in the atmosphere (Lambert, 1980; Fowler, 2004; Zahnle, 2006; Rey and Houseman, 2006). The possible extensive cover of greenstones on the surface could have also thermally insulated the granitic crust (Rey et al., 2003). All of these factors would have resulted in weaker crust and resultant broad ductile deformation of the Archean crust (West and Mareschal, 1979).

Metamorphic facies of granite-greenstone terrains varies generally from greenschist to amphibolite-facies or medium to high temperature and low to medium pressure. Metamorphic conditions generally increase from greenschist-facies within the greenstone belts to amphibolite-facies towards the edge of the granitic bodies (Anhauesser, 1969). Evidence for blueschist-facies metamorphism, diagnostic of modern

arc-terrane accretion, has not been documented in any Archean craton. However, the lack of blueschist-facies rocks could result from a lack of sodic–rich volcanic rocks, or to later overprinting, rather than to unique thermal conditions during the Archean (Anhauesser et al., 1969).

### 2.2 Superior Province

The Archean Superior Province is the location of numerous studies focused on granite-greenstone terrain development. Archean rocks in the Superior Province, not unlike other Archean cratons, consist of large elliptical granite bodies surrounded by metavolcanic and metasedimentary rocks (Fig. 1). Early studies of granite-greenstone terrains development in Archean cratons, including the Superior Province, invoked sagduction/diapirism (McGregor, 1951; Anhauesser, 1969; Hooper and Ojakangas, 1971; Sims, 1979; Mareschal and West, 1980). Based on mapping in northeastern Minnesota, Sims (1979) concluded that the upright folding of volcanic packages was contemporaneous with emplacement of granitic bodies located to the north and south of the Vermilion District consistent with sagduction/diapirism.

With the acceptance of modern plate tectonics, however, research in the Superior Province has favored arc-terrane accretion. This new interpretation is based on data from: 1) seismic images, which can be interpreted to record remnant subducted plates (Calvert et al., 1995), 2) radiometric ages of 3.0 Ga in the northern Sachigo subprovince to 2.7 Ga in the southern Abitibi and Wawa subprovinces, which infer units young progressively from north to south (Card, 1990; Kimura et al., 1993), and 3) rock units that could correlate lithologically with accretionary wedges and an arc-accretion tectonic

setting (Percival and Williams, 1989). Dextral transpression by way of northwest-directed oblique convergence evolved as the favored tectonic process for the Superior Province in northeastern Minnesota (Tabor and Hudleston, 1991; Jirsa et al., 1992; Czech and Hudleston, 2002).

Although the two hypotheses in this paper are discussed separately, recently some research suggests that both processes could have occurred in the Superior Province. In Canada, for example, workers conclude that vertically dominated tectonism evolved into dominantly horizontal tectonism over time (Bedard et al., 2003; Lin, 2005; Parmenter et al., 2006). Lin (2005) states that vertical and horizontal deformation mechanisms do not have to act exclusively of each other. Granite-greenstone terrains could have resulted from dip-slip and strike-slip displacement by way of sagduction/diapirism that may have transitioned to the arc-terrane accretion process with time.

### 2.3 Northeastern Minnesota

The Superior Province, northeastern Minnesota, is a broad region of volcanic rocks bordered to the north and south by granitic complexes. The Superior Province in northeastern Minnesota is comprised of the Quetico Subprovince to the north and the Wawa Subprovince to the south. The Vermilion District is located within the Quetico and Wawa subprovinces.

#### *Vermilion District*

The Vermilion District contains, from north to south, the Vermilion Granitic Complex, Newton Lake/Bass Lake Formation, Knife Lake Group/Vermilion Lake Formation, the Soudan Iron Formation separating the Lower and Upper Members of the

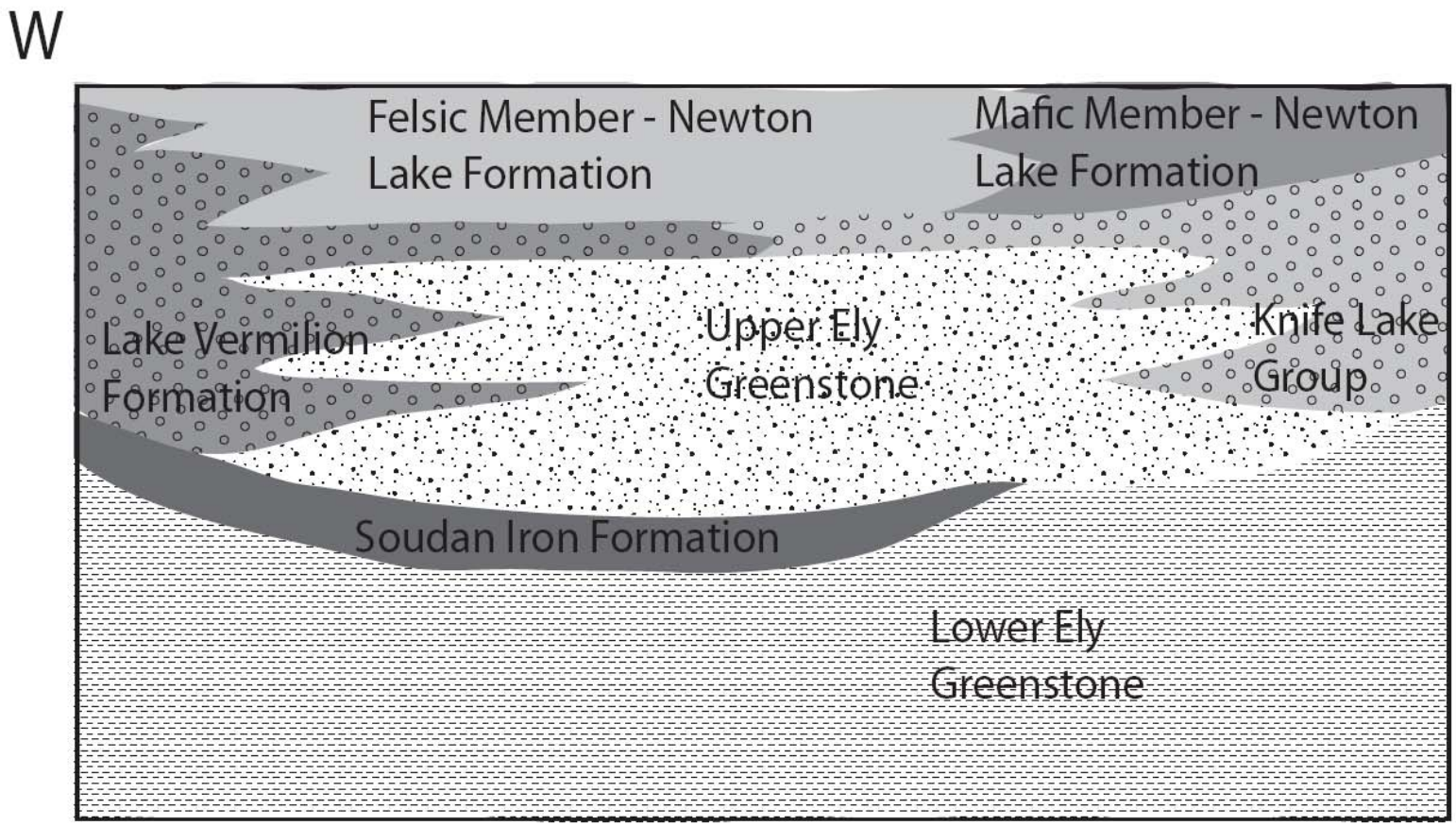


Figure 4. Cartoon cross-section of the Vermilion greenstone belt showing reconstructed stratigraphic relationships, pre-folding and faulting (After Schulz, 1980). Cartoon refers to box location in figures 1 and 2.

Ely Greenstone, and the Giants Range Batholith (Fig. 4). Figure 4 illustrates a cross-section through the Vermilion District with each of these units in stratigraphic order, and referenced to its equivalent stratigraphy within each of the hypotheses outlined in figures 2 and 3.

The Vermilion Granitic Complex includes the Lac La Croix Granite, granite-rich and biotite-rich migmatites, biotite and amphibolite schists, metagabbro, metabasalt, and the Wakemup and Burntside trondhjemites. The Newton Lake Formation/Bass Lake Formation contains protoliths of gabbro diabase pyroxenite and periodite, basalt flows, banded iron formation, and volcanic rocks of clastic, calc-alkalic and tholeittic composition. The Knife Lake Group/Vermilion Lake Formation consists of protoliths of felsic tuff, conglomerate and felsic volcanic rocks. The Upper Ely Greenstone member contains metadiabase and metagabbros, tholeiitic pillowed basalt and calc-alkalic volcanic rocks. The Lower Ely Greenstone member includes tholeittic basaltic and calc-alkalic volcanic rocks. The Giants Range Granite is a quartz monzonite (Jirsa and Miller, 2004). The calc-alkalic volcanic rocks of the Upper Ely Greenstone Member may be more similar to volcanic rocks of the Knife Lake Group (Green et al., 1966). The Newton Lake Formation and Knife Lake Group may be equivalent lithologically to the Bass Lake Formation and the Vermilion Lake Formation of the western Vermilion District. The Vermilion fault system trends E-W and displaced volcanic rock units ~17 km (Sims, 1976) (Fig. 5).

*Shagawa Lake shear zone*

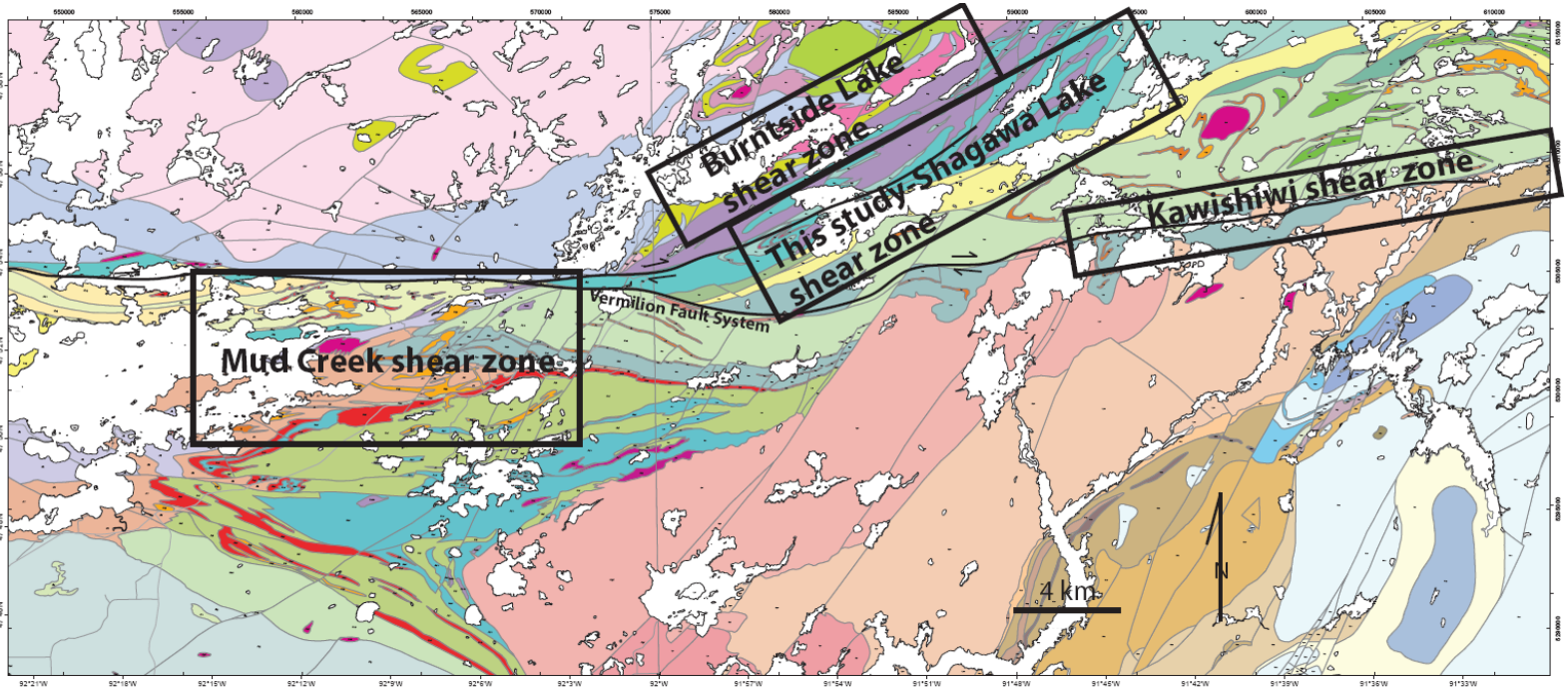


Figure 5. Map of the Vermilion District showing the location of other shear zones being studied in the region and the the location of the Vermilion Fault System. This figure is in reference to the broad study area in Figure 1.

The Shagawa Lake shear zone is one in a series of SW-NE trending shear zones in the Vermilion District, including the Mud Creek, Burntside Lake and Kawishiwi shear zones (Fig. 5). The shear zones of the Vermilion District occur within a volcanic and volcaniclastic greenstone belt bordered to the south and north by granitic bodies, the Giants Range Batholith and Vermilion Granitic Complex, respectively. The greenstone belt includes the Newton Lake Formation, Knife Lake Group and Lower and Upper Ely Greenstone.

Previously the Shagawa Lake shear zone had only been structurally and kinematically studied in areas around Shagawa Lake and farther east in Canada (Bidwell, 1988; Bauer and Bidwell, 1990; Wolf, 2006). The Shagawa Lake shear zone is interpreted to have undergone northwest-directed subduction resulting in dextral transpression across an east-striking convergent margin (Bidwell, 1988; Bauer and Bidwell, 1990) but may have undergone sinistral displacement in Canada (Wolfe, 2006). Displacement is interpreted to be top to the southeast. Dextral oblique shear is the dominant interpretation for the Shagawa Lake shear zone.

Deformation within granite-greenstone terrains occurs mostly within the greenstone belts. Shear zones within these greenstone belts are a prominent deformational feature and offer an ideal location to perform structural analyses within granite-greenstone terrains.

## 3. Methods

A structural and kinematic analysis was conducted within the Shagawa Lake shear zone by performing field and laboratory work. Field work included collection of foliation and Le data, and oriented samples for microstructrual analysis. Microstructural analysis and creation of structural and kinematic maps was conducted using optical microscope and computer laboratories.

### 3.1 Field Work

During approximately three months of field work, foliation and Le orientations, and oriented samples were collected along and across the Shagawa Lake shear zone. North-south transects on the west, central and east portion of the study area and along lakes and roads were the focus of data collection. 201 oriented samples were collected in the field. Rock samples were oriented in reference to the foliation and Le (Hansen, 1990). Geologic data were recorded at every field spot including the outcrop location in UTM and latitude/longitude coordinates, rock type, foliation and Le orientation (if present) and any other consistent and relevant structural features such as tension gashes and kink bands.

In general foliations range from continuous or spaced cleavages and are defined by compositional layering and flattened or aligned minerals. Foliations form during deformation and metamorphism. Le is defined by aggregates or preferred orientation of minerals on the foliation plane. Foliated rocks without an Le are considered S-tectonites and foliated rocks with an Le are classified as L-S tectonites. Pitch is the angle measured

on the foliation plane from the strike of the foliation to the plunge of the Le. Le is an indication of the displacement direction during deformation.

Tension gashes and kink bands were documented at outcrop scale. The location, rock type, orientation and abundance of each were recorded in relation to the foliation and Le. Tension gashes form perpendicular to the stretching direction. In the case of the Shagawa Lake shear zone, tension gashes typically formed perpendicular to Le, indicating that Le likely formed parallel to the direction of tectonic transport. No shear sense indicators were confidently interpreted in the field due to poor 3-D outcrop views. Because, Le-perpendicular tension gashes indicate Le may have formed parallel to tectonic transport by stretching, the motion plane is likely parallel to Le and perpendicular to tension gashes. Roadside exposures and shorelines of Shagawa Lake and Fall Lake provided the best outcrops.

### 3.2 Laboratory Work

Laboratory work was comprised mainly of structural and microstructural analysis. Orientation of bedding, foliation and Le were compiled on equal-area lower-hemisphere stereonets and thin sections were made for petrographic and microstructural analysis. Structural and kinematic data are illustrated in foliation trajectory and Le pitch maps. All field data was compiled and analyzed in GIS computer laboratories and on optical microscopes.

*Structural and Kinematic Maps*

Maps were created using ArcGIS 9.2™ and Adobe Illustrator CS3™ and stereonets were created using Stereowin 1.2©. The MN Geological Survey M-148 map

was used as a base map in ArcGIS (Jirsa and Miller, 2004). Foliation, Le orientation, bedding and thin section locations were imported as attributes into ArcGIS from Excel tables. All data are referenced to the NAD 1983 Zone 15T UTM coordinate system. The Excel data tables were represented as layers on top of the geology.

The geology of the shear zone was generalized based on the M-148 map and imported into Adobe Illustrator CS3. Within CS3, layers representing foliation trajectory, Le pitch and kinematic data at the location of each thin section layer are compared with the general geology. The foliation trajectories connect similar foliation strike with trajectory lines along the shear zone. Le pitch was graphed on a histogram and divided into five groups based on orientation.

Kinematic data are illustrated on equal-area stereonets that represent the shear sense interpretations in the context of the individual rock sample foliation and Le data. Kinematic data are illustrated as south-side-up dip-slip, north-side-up dip-slip, or sinistral strike-slip shear.

## 4. Results

This structural and kinematic analysis of the Shagawa Lake shear zone focuses on an ~18 km long and ~3-4 km wide portion of the shear zone (Plate 1). The Shagawa Lake shear zone is defined by an east-northeast striking and steeply-dipping foliation. The shear zone is comprised of meta-volcanic L-S tectonites that separate granite bodies to the north and south.

### 4.1 Structural Data

Foliation and Le were measured in the field and additional foliation, Le, and bedding measurements were gleaned from the Shagawa Lake, Ely and Gabbro Lake MGS quadrangles (Plate 1A and Fig. 6) (Sims and Mudrey, 1978; Green and Schulz, 1982; Green et al., 1966). All measurements were plotted on an equal-area lower-hemisphere stereonet. Maps of foliation trajectory and Le pitch were compiled.

Foliation generally strikes east-northeast and is dominantly steeply-dipping to the south. The average foliation ($065^{o}$, $80^{o}$ S) generally parallels bedding ($060^{o}$, $85^{o}$ S). Foliation exists throughout the extent of the study area (Plate 1). Foliation measurements are widely distributed in space within the shear zone. Regardless of rock lithologies, along and across the shear zone the foliation consistently strikes to the east-northeast. Foliation is defined within the shear zone by compositional layering, and by the alignment of chlorite, actinolite, epidote, feldspar, mica, and calcite. Compositional layering may have been relic bedding but is considered foliation in this study.

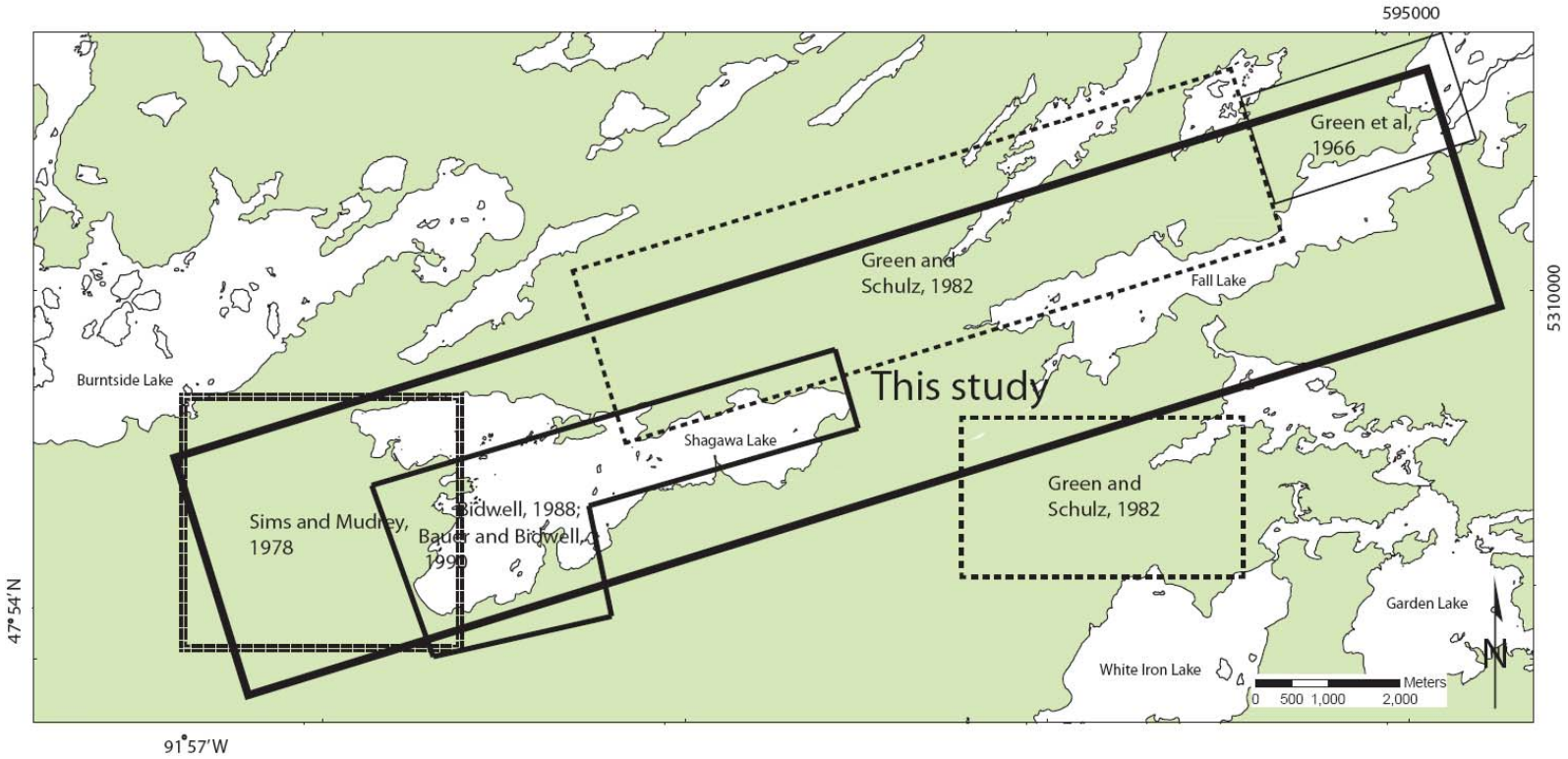


Figure 6. Map of the Shagawa Lake shear zone illustrating data sources and other studies referred to in this study.

Foliation trajectories highlight the general foliation strike from SW to NE within the study area. Foliation trajectories are mainly straight, and parallel lithologic contacts. Foliation trajectories illustrated in this study do not constrain the location of the Shagawa Lake shear zone.

Le, which lies within the foliation, is defined by grain and mineral stretching lineation which commonly exist locally and pervasively throughout outcrops of all lithologies (Plate 2a). Le is commonly defined by the alignment of chlorite, actinolite, mica and epidote on the foliation plane. Le delineates two populations marked by dip-slip and strike-slip orientation within the foliation. Le dominantly plunges moderately to steeply to the east and west (90 ±30) with subsidiary shallowly plunging Le to the east and west (15 ±10) (Plate 1).

Given the steep dip of foliation, Le orientation is perhaps most easily visualized using pitch (Plate 3). Pitch is the angle on the foliation plane measured from the strike of the foliation to a line. Although pitch is traditionally noted as the acute angle from strike I used a different convention here. Because foliation strikes SW-NE and is steeply-dipping, the pitch of Le is measured from east ($0^o$) to west ($180^o$) (Plate 3). A histogram of Le pitch illustrates the variability of pitch within the shear zone and highlights populations of similar orientation (Plate 3A). Based on the modal distribution, five Le orientation domains are apparent. These include three dip-slip domains: steeply-plunging ($60^o$-$120^o$), moderately-plunging to the east ($35^o$-$60^o$) and west ($145^o$-$120^o$), and two strike-slip domains: shallowly-plunging to the east ($0^o$-$35^o$) and west ($180^o$-$145^o$). The strike-slip domains are considered a single domain given their orientation about horizontal. Pitch is everywhere steeply-plunging except where there are zones of

obliquely- to shallowly-plunging Le (Plate 3). Le orientation domains are distributed within the shear zone with no obvious pattern. Shallowly and obliquely plunging Le to the east and west are located in zones with no preferred orientation or location within the shear zone. Although strike-slip Le is less dominant and less pervasive than dip-slip Le, dip-slip and strike-slip Le occur locally in the same rock.

Tension gashes are marked by thin fractures that extend tens of centimeters within outcrops. Tension gashes are most common in greenstone and metadiabase lithologies and are commonly filled with calcite. Tension gashes typically cut the foliation plane perpendicular to Le (Plate 2i).

### 4.2 Petrographic and Microstructural Analysis

Petrographic and microstructural analysis of thin sections from within the Shagawa Lake shear zone indicate greenschist facies metamorphic conditions and kinematic patterns that can be accounted for by three deformation events.

*Petrography*

Petrographic analyses included identification of minerals, metamorphic facies and protoliths (Table 1). For each thin section I identified the mineral assemblage, relative mineral abundances and trace minerals. The minerals are identified as metamorphic, detrital or relic. Metamorphic facies and possible protolith of the samples are extrapolated based on mineral assemblage present within each thin section. Common minerals are chlorite, actinolite, epidote, clinozoisite, plagioclase, quartz, muscovite, pyrite, calcite and siderite (Table 1). Some combination of chlorite, actinolite, epidote, mica and calcite typically define foliation. The typical metamorphic

Table 1. General petrographic data including mineral and metamorphic mineral assemblages

| | | | | | Mineral Assemblage | | | | | | | | | | | | | | | |
|---|---|---|---|---|---|---|---|---|---|---|---|---|---|---|---|---|---|---|---|---|
| Sample # | Northing | Easting | Rock Name | Grain size | Wm | Chl | Act | Amp | Ep | Cz | Cc | Sid | Qtz | Py | Opq | Plag | Fs | Ox | Pyr | Metamorphic Grade | Protolith |
| 003 | 578534 | 5307078 | greenstone or black phyllite | Fine to Medium | | X | X | | | | X | | R? | | X | X | | | | Greenschist | Mafic Volcanic |
| 007 | 578351 | 5307826 | greenstone to gray phyllite | Fine to Medium | | X | X | | | | X | X? | tr | X | | X | | | | Greenschist | Mafic Volcanic |
| 010 | 582822 | 5308580 | greenstone | Fine | | X | X | | | | X | | X | | X | X | | | | Greenschist | Mafic Volcanic |
| 021 | 595391 | 5311490 | greenstone | Fine to Medium | | X | | | X | | X | | | | X | X | | | | Greenschist | Volcanic |
| 022-B | 594065 | 5310493 | gray schist | Fine to Medium | X | X | X | | | | X | | X | X | | X | tr | | | Greenschist | Felsic Volcanic |
| 025 | 594750 | 5310732 | Gray schist | Fine | X | X | | | | | | | D? | tr | | X | | X | | Greenschist | Felsic Volcanic /Greywacke? |
| 025-2 | 594750 | 5310732 | Gray schist | Fine | X | X | | | | | X | | D? | tr | | X | | | | Greenschist | Felsic Volcanic /Greywacke? |
| 030 | 585246 | 5308498 | greenstone | Fine | | X | | | tr | | X | | X | X | | | | | | Greenschist | Volcanic |
| 032-1 | 588960 | 5309681 | green schist or greenstone | Fine | X | X | | | tr | | X | | X | X | | X | | | | Greenschist | Mudstone/Greywacke |
| 032-2 | 588960 | 5309681 | green schist or greenstone | Fine | X | X | | | tr | | X | | X | X | | X | | | | Greenschist | Mudstone/Greywacke |
| 034-B | 579701 | 5305765 | metabasalt | Fine to Medium | | X | | R? | X | X | X | | X | X | | X | | | | Greenschist to Amphibolite (?) | Mafic Volcanic |
| 037 | 578967 | 5306001 | Felsic to intermediate tuff | Fine to Coarse | | X | X | | X | | | | X | | X | X | | | | Greenschist | Felsic Volcanic |
| 043 | 580849 | 5306451 | metagabbro | Fine to Medium | | X | X | R | X | | | X? | X | | | X | | | | Greenschist | Basalt |
| 043-S | 580849 | 5306451 | metagabbro | Fine to Medium | | X | X | R | X | | X | X? | | | | X | | | | Greenschist | Basalt |
| 044 | 579076 | 5304469 | gray schist | Fine | X | X | | | | | X | X? | | | X | X | | X | | Greenschist | Mudstone/Greywacke |
| 049 | 590097 | 5310241 | greenstone | Fine | | tr | X | | X | | | | X | | X | X | | | | Greenschist | Mafic Volcanic |
| 057-S | 588730 | 5309669 | greenstone | Fine | | X | | | X | | X | | X | | X | | | | | Greenschist | Volcanic pyroclastic deposit? |
| 072 | 587738 | 5309341 | greenstone or green phyllite | Fine | | X | X | | X | | | | tr | | tr | | | | | Greenschist | Mafic Volcanic |
| 076 | 582859 | 5308653 | green phyllite | Fine | X | X | X | | | | X | | X | | X | X | | X | | Greenschist | Mafic Volcanic |
| 090-B | 591293 | 5310713 | greenstone | Fine to Medium | | X | X | | X | | | | | | | X | | | D | Greenschist | Mafic Volcanic |
| 097 | 577785 | 5307596 | greenstone to gray phyllite | Fine | | X | X | | X | X | X | | X | X | | | | | | Greenschist | Mafic Volcanic |
| 099-C | 586025 | 5308724 | greenstone to green phyllite | Very Fine | X | X | X | | | | | | X | X | | X | | tr | | Greenschist | Mafic Volcanic |
| 101 | 578351 | 5307826 | greenstone | Fine to Coarse | | X | X | | | | X | | | | | X | | | | Greenschist | Mafic Volcanic |
| 106 | 586025 | 5308725 | greenstone | Fine | | X | | | X | | | | | | X | X | | | | Greenschist | Mafic Volcanic |
| 109 | 587050 | 5308817 | gray schist | Fine to Medium | X | X | X | | | | X | | | X | | X | | X | | Greenschist | Mudstone/Graywecke |
| 114 | 586720 | 5309186 | gray phyllite to gray schist | Fine | | X | | | X | X | | | | | | | | | | Greenschist | Felsic Volcanic |
| 129 | 589359 | 5309811 | green schist or greenstone | Fine | | X | | | X | X | X | X? | | | X | X | | X | | Greenschist | Mafic volcanics |
| 135 | 590037 | 5309878 | gray schist | Fine | X | X | | | | | X | | X | X | | X | | | | Greenschist | Felsic Volcanic? |
| 138 | 590622 | 5310224 | greenstone to green schist | Fine | X | X | | | | | X | X? | X | | X | X | | X | | Greenschist | Felsic to Mafic Volcanic? |
| 140 | 591289 | 5309593 | gray phyllite | Fine | | tr | X | | | | X | X?/tr | | | X | X | | | | Greenschist | Felsic to Mafic Volcanic |
| 142 | 586895 | 5308243 | gray phyllite | Very Fine | | | X | | | | X | | X | | X | X | | | | Greenschist | Volcanic |
| 144 | 583799 | 5307585 | gray schist | Fine | X | X | X | | | X | X | | | X | | X | | tr | | Greenschist | Mudstone/Greywacke |
| 157 | 589540 | 5309056 | gray schist | Fine to Medium | X | X | | | | | X | X? | | | X | R | | X | | Greenschist | Mudstone/Greywacke |
| 164 | 580805 | 5307940 | greenstone | Fine | | X | | | X | | tr | | X | | X | X | | | | Greenschist | Mafic Volcanic |
| 167 | 582155 | 5307713 | metadiabase | Fine | | X | X | | X | | X | | X | | X | X | | | | Greenschist | Mafic Volcanic |
| 167-S | 582155 | 5307713 | metadiabase | Fine | | X | X | | X | | X | | X | | X | X | | | | Greenschist | Mafic Volcanic |
| 170-B | 581650 | 5306329 | felsic to intermediate phyllite | Fine to Medium | | tr | X | R | | | X | | | | tr | X | | | | Greenschist | Felsic Volcanic |
| DA-2 | 586638 | 5308719 | greenstone or gray schist | Fine | | X | X | | tr | | X | X? | X | | X | X | | X | | Greenschist | Felsic to Mafic Volcanic |

In microscope view coarse grain size=>0.4mm, medium grain size=0.4mm-0.25mm, and fine grain size= <0.1mm. Wm=White mica, Chl=chlorite, Cz=Clinozoisite, Cc=Carbonate, Sid=Siderite, Act=actinolite, Amp=Amphibole, Ep=epidote, Ox=Oxide, Qtz=Quartz, Py=Pyrite, Opq=Opaque, Plag=Plagioclase, Fs=Feldspar, Pyroxene=Pyr, D=detrital, R=relic, tr=trace

mineral assemblage of chlorite, actinolite, epidote and clinozoisite indicates greenschist-facies metamorphic conditions. Protoliths are commonly basalt, volcanic deposits, and mudstone/greywacke. White mica is associated with mudstones/greywackes and chlorite and actinolite are common minerals within the mafic volcanic rocks such as greenstone. It is unclear if the amphibole within some mafic volcanic rocks represents a relic or metamorphic phase. Veins that crosscut foliation are typically filled with quartz or calcite; quartz and calcite occasionally occur in the same vein. Calcite and possibly siderite are abundant within the matrix and could represent diagenic cement or metasomatic processes. Metasomatism involves the infiltration and/or diffusion of fluids or material through fluid and solid phases (Winter, 2001). During metasomatism, carbonate from a $CO_2$-rich Archean environment could have infiltrated the rocks during deformation and metamorphism. Seafloor metamorphism is a likely environment for high $CO_2$ partial pressures and would have affected underwater volcanic flows. Metasomatism can operate as submarine hydrothermal metamorphism or at the low to medium P/T conditions characteristic of granite-greenstone terrains. There could have been a transition from a submarine to burial metamorphic environment.

*Motion plane location*

In order to perform kinematic analyses I determined the location of the motion plane. The motion plane is defined as the plane that contains a discernable asymmetric fabric. In general, the motion plane lie normal to foliation, parallel to Le; the vorticity axis lies perpendicular to Le. Le can also form parallel to vorticity by rolling but this is rare (Fig. 7a) (Passchier and Trouw, 2005).

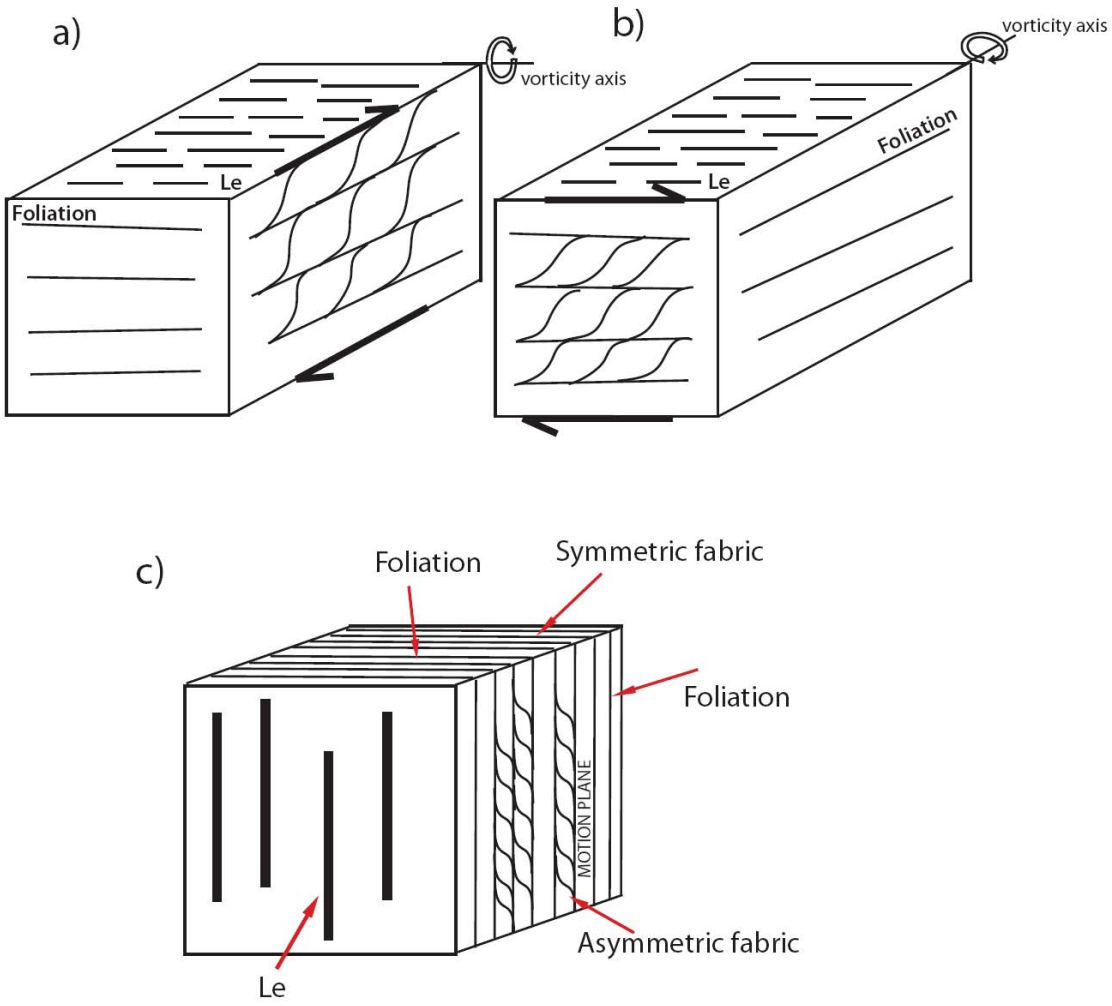


Figure 7. Schematic diagram of possible non-coaxial shear sense orientations. a) shear sense orientation with vorticity axis parallel to Le; this is a rare case; b) shear sense orientation with vorticity axis perpendicular to Le; c) Location of fabric asymmetry and motion plane for Shagawa Lake shear zone L-S tectonites in reference to the Le on the foliation plane based on microstructures. (a and b after Passchier and Trouw, 2005)

The motion plane was determined by cutting three suites of thin sections parallel and perpendicular to the Le from three L-S tectonites samples. These thin sections were examined for the presence or lack of a dominant asymmetric fabric (Fig. 7).

Sections cut normal to foliation and parallel to Le show asymmetric fabric, whereas sections cut normal to foliation and Le display symmetric fabric (Fig. 7c and Plate 2d). Sections cut parallel to Le display kinematic indicators including S-C fabric, consistent quartz strain shadows around pyrite or opaque grains and/or a dominant grain shape preferred orientation of minerals aligned with S-C fabrics (Plate 2c, g-i). These relations are consistent with L-S tectonite formation via non-coaxial shear with the motion plane normal to foliation and Le. Two suites of thin sections cut parallel and normal to Le are consistent with non-coaxial shear. One sample, 032, showed asymmetric fabrics in both thin sections.

Sample 032 contains an interesting relationship that is important to discuss in the context of deformation style within the Shagawa Lake shear zone. Sample 032 displays a dip-slip Le within the foliation plane (246, 82 NW). Sample 032 was cut both parallel and perpendicular to a dip-slip Le (083, 65). Surprisingly, asymmetric fabrics occur within both planes (Plate 2e-f) (Fig. 8). The section parallel to Le displays a pervasive S-C fabric, whereas the section perpendicular to Le has a less well developed S-C fabric. This relationship is different than the other samples cut parallel and perpendicular to one Le (Plate 2c-d).

One explanation for the fabric patterns in sample 032 could be that the overall displacement direction is recorded in the section parallel to Le, however small increments of lateral horizontal shearing left and right created less developed opposing S-C fabrics in

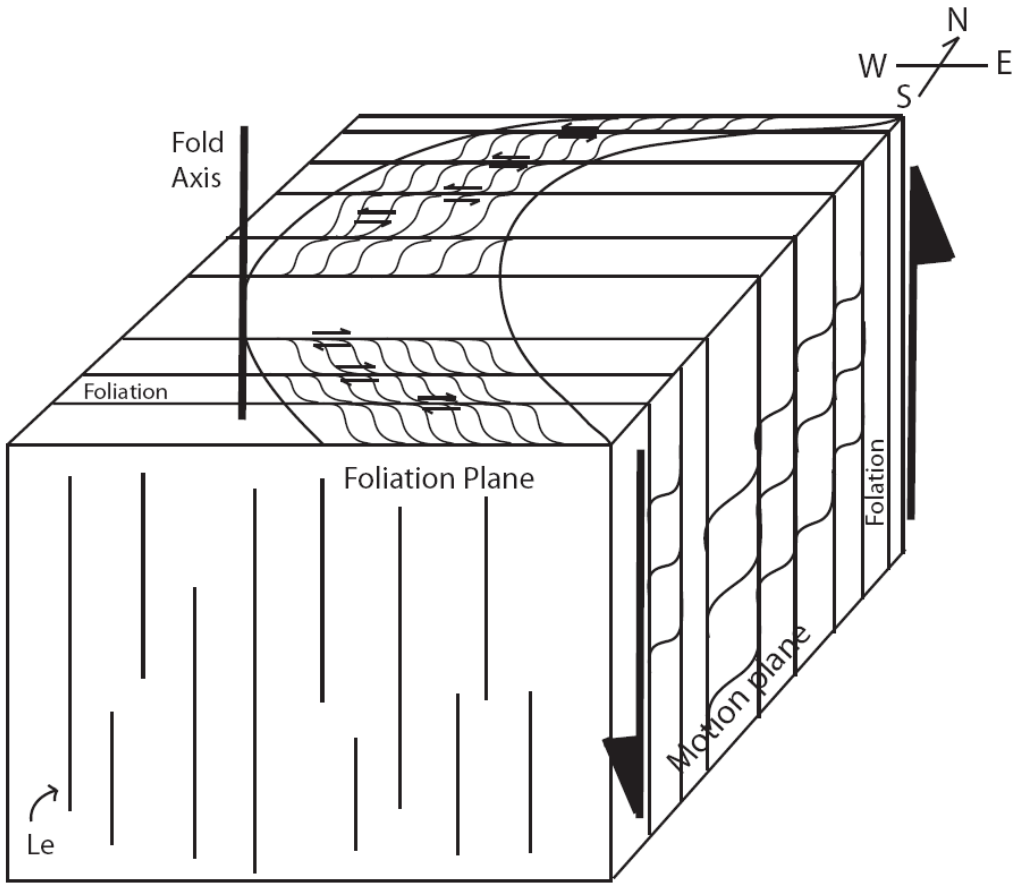


Figure 8. Cartoon block diagram illustrating fabric geometries and possible kinematic relationship in sample 032. The dominant deformation event is dip-slip shear in the motion plane parallel to the Le. The plane perpendicular to Le records incremental subsidary slip within and during the dominant dip-slip shearing. The fold axis parallels Le.

the section perpendicular to Le (Fig. 8). Sample 032 shows dextral shear sense in the section perpendicular to Le; however folds with axes parallel to Le, occur at the outcrop scale; the plane perpendicular to foliation and Le represents the axial profile view. These folds might accommodate small incremental movement within the more pervasive oblique- to dip-slip deformation.

*Microstructural Data*

Of the 201 oriented samples, 47 were cut for thin sections, made by Vancouver Petrographics Ltd. and Spectrum Petrographics Inc. Forty-four sections provide motion plane views and three sections are normal to foliation and Le. For samples with both dip-slip and strike-slip Le, sections were cut parallel to both Le orientations.

Each thin section was analyzed for microstructures indicative of shear sense (Fig. 9). Shear sense interpretations within the motion plane, normal to foliation and parallel to Le, proved challenging. Of the 49 thin sections, I was able to, with varying degrees of confidence, interpret 39 for shear sense. The most useful shear sense indicators include S-C fabrics, strain shadows and fibrous veins (Table 2 and Plate 2f-i). Clastic and volcanic rocks of the Knife Lake Group and Newton Lake Formation yielded the best microstructural kinematic indicators. Ely Greenstone was not a reliable rock to analyze for shear sense indicators because it contains abundant pillow basalts and shear can localize along the pillow boundaries. This localization of shear makes it difficult to interpret shear sense indicators because asymmetry is not distributed within the rock.

Although quartz was present in many of the thin sections, it did not generally exhibit obvious lattice preferred orientation, likely due to pinned grain boundaries. Quartz occasionally occurs with calcite in fibrous veins and the calcite preferentially

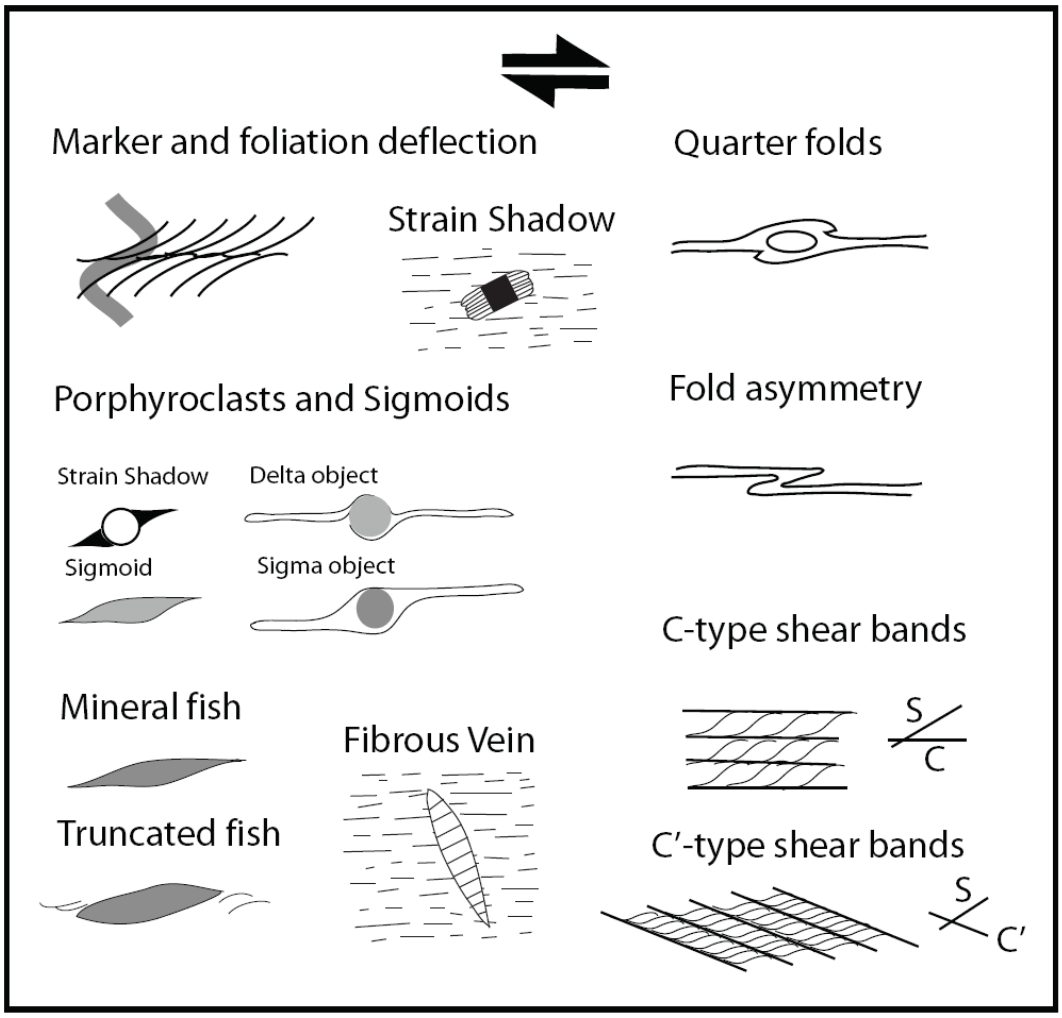


Figure 9. Common types of shear sense indicators. All indicators show dextral shear sense. Modified from Passchier and Trouw (2005).

**Table 2. Microstructural kinematic data compiled from each of 34 thin sections analyzed. Each section is cut parallel to Le.**

| Sample # | Northing | Easting | Foliation | Lineation | Pitch (from E) | Direction facing when looking at section (cover sheet up) | Shear Sense | Confidence (1 is low) | Shear Sense Indicators | Foliation and S-C Defined by | | | | | | | Pitch |
|---|---|---|---|---|---|---|---|---|---|---|---|---|---|---|---|---|---|
| | | | | | | | | | | Wm | Chl | Act | Ep/Cz | Cal | Plag | Opq | |
| 043-S | 580849 | 5306451 | 099, 66 S | 105, 13 | 15 | UP | Sinistral | 3 | S-C | | X | | | | | | 0-35 and 180-146 |
| 025-2 | 594750 | 5310732 | 052, 89 SE | 231, 17 | 163 | UP | Sinistral | 4 | Strain shadows | X | | X | | X | | | |
| 072 | 587738 | 5309341 | 075, 83 SE | 084, 51 | 52 | W AND DOWN | South up | 3 | S-C | | X | X | | | | | 36-60 |
| 076 | 582859 | 5308653 | 039, 46 NW | 357, 37 | 53 | W | South up | 2 | S-C and strain shadows | | X | X | | X | | | |
| 170-B | 581650 | 5306329 | 243, 86 SE | 070, 59 | 59 | W AND DOWN | South up | 3 | S-C | | | X | | | | X | |
| DA-2 | 586638 | 5308719 | 071, 76 SE | 085, 46 | 48 | E AND SLIGHTLY UP | North up | 2 | S-C | | X | | | X | | X | |
| 032-1 | 588960 | 5309681 | 246, 82 NW | 083, 65 | 54 | E AND SLIGHTLY UP | North up | 5 | S-C | X | | X | | X | | | |
| 109 | 587050 | 5308817 | 274, 77 S | 107, 62 | 54 | E AND UP | North up | 2 | S-C | | X | X | | X | | X | |
| 021 | 595391 | 5311490 | 242, 74 NW | 082, 50 | 58 | E AND SLIGHTLY DOWN | North up | 3 | S-C | | X | | | X | | X | |
| 044 | 579076 | 5304469 | 216, 67 N | 042, 56 | 64 | W AND DOWN | South up | 4 | S-C | X | | X | | | | | 61-120 |
| 049 | 590097 | 5310241 | 057, 72 SE | 089, 58 | 64 | W AND DOWN | South up | 2 | S-C and tension fractures | | X | | X | | | | |
| 157 | 589540 | 5309056 | 036, 76 SE | 048, 64 | 66 | W | South up | 4 | S-C and actinolite mats | X | | X | | | | X | |
| 043 | 580849 | 5306451 | 099, 66 S | 143, 58 | 68 | W AND SLIGHTLY DOWN | South up | 1 | S-C and chlorite mats | | X | | | | | | |
| 090-B | 591293 | 5310713 | 036, 72 NW | 358, 62 | 68 | E | South up | 4 | S-C-C' | | X | X | | | | | |
| 135 | 590037 | 5309878 | 040, 30 SE | 135, 30 | 86 | W | South up with cross-cutting North up | 3 | S-C actinolite mats | | X | X | | X | | | |
| 007 | 578351 | 5307826 | 090, 59 S | 180, 59 | 90 | W | South up | 3 | S-C and strain shadows | | X | X | | X | | | |
| 097 | 577785 | 5307596 | 080, 54 S | 170, 54 | 90 | E | South up | 3 | S-C and strain shadows | | X | | X | X | | | |
| 101 | 578351 | 5307826 | 082, 58 S | 172, 58 | 90 | W | South up | 4 | S-C | | X | X | | X | | | |
| 030 | 585246 | 5308498 | 231, 71 SE | 169, 69 | 100 | W AND UP | South up | 3 | S-C and strain shadows | | X | | | X | | | |
| 022-B | 594065 | 5310493 | 248, 74 SE | 210, 62 | 109 | W AND UP | South up | 3 | S-C | X | X | X | | | | X | |
| 106 | 586025 | 5308725 | 264, 80 NW | 264, 80 | 116 | W AND UP | South up | 3 | S-C | | X | X | | | | | |
| 164 | 580805 | 5307940 | 235, 87 SE | 063, 69 | 69 | E | North up | 1 | S-C and C' in chlorite | | X | | | X | | X | |
| 142 | 586895 | 5308243 | 088, 72 SE | 110, 56 | 80 | E | North up | 2 | S-C | | | | | | | | |
| 144 | 583799 | 5307585 | 074, 73 SE | 194, 72 | 81 | E | North up | 3 | S-C | X | X | X | | | | | |
| 140 | 591289 | 5309593 | 210, 83 SE | 246, 80 | 98 | E | North up | 3 | S-C, tension fractures and strain shadows | | X | | | X | | X | |
| 037 | 578967 | 5306001 | 093, 82 S | 218, 80 | 95 | E | North up | 2 | S-C | | X | X | | | | | |
| 034-B | 579701 | 5305765 | 268, 65 N | 330, 62 | 102 | E | North up | 1 | S-C and C' in chlorite | | X | | | | | | |
| 010 | 582822 | 5308580 | 235, 70 SE | 194, 63 | 103 | E | North up | 3 | S-C and strain shadows | | X | X | | | | X | |
| 114 | 586720 | 5309186 | 239, 74 SE | 190, 64 | 104 | E | North up | 3 | S-C | | X | | | X | | | |
| 099-C | 586025 | 5308724 | 253, 83 N | 268, 65 | 114 | E AND SLIGHTLY DOWN | North up | 3 | S-C | X | | X | | | | | |
| 138 | 590622 | 5310224 | 245, 75 NW | 284, 55 | 122 | W AND UP | South up with cross-cutting North up | 2 | S-C and chlorite mats | | X | | | | X | | 121-145 |
| 129 | 589359 | 5309811 | 242, 73 SE | 218, 52 | 125 | E AND DOWN | North up | 3 | S-C and chlorite mats | | X | | | X | | | |
| 057-S | 588730 | 5309669 | 249, 87 SE | 246, 33 | 129 | E AND DOWN | North up | 3 | S-C and tension fractures | | X | | | X | | | |
| 003 | 578534 | 5307078 | 255, 74 S | 242, 38 | 140 | E AND DOWN | North up | 3 | S-C and strain shadows | | X | | | X | | | |

Wm=White Mica, Chl=Chlorite, Act=Actinolite, Ep=Epidote, Cz=Clinozoisite, Cal=Calcite, Plag=Plagioclase, Opq=Opaque.

accommodates more of the deformation in the fractures, preventing quartz from deforming. In addition, quartz was not abundant in many of the thin sections.

S-C fabrics are the most common and well developed microstructural shear sense indicators within Shagawa Lake shear zone L-S tectonites. Chlorite and actinolite commonly defined both S and C planes. S-C fabrics were best developed in chlorite- and mica-rich metavolcanic and metasedimentary rocks of the Knife Lake Group and Newton Lake Formation. S-planes are penetrative, or closely-spaced, whereas C-planes are more widely spaced. S-planes are transected by C-planes at an angle and together they create an S-C fabric. The angle between the S and C planes defines the sense of non-coaxial shear rotation. The infinitesimal strain ellipse is elongate along S-planes and C-planes are parallel to slip planes (Plate 2e, f, g). S-planes are defined by the alignment of chlorite, epidote, feldspar and/or mica and the C-planes are commonly defined by actinolite and/or calcite (Plate 2c, e, f, g). Sample 090-B displays S, C, and C' shear planes (Plate 2g). C' planes are spaced and form after S and C shear bands with continued deformation. Within sample 090-B, the alignment of pyroxene and actinolite define S planes. The alignment of actinolite and chlorite define C and C' planes. A fracture in the section formed when continued shearing caused the rock to transition from ductile to brittle deformation to accommodate stress. The fracture opened along the $X_i$ axis of the infinitesimal strain ellipse, also known as the direction of maximum elongation. Chlorite within the fracture is aligned parallel to $X_i$. Both the S-C-C' fabric and fracture display sinistral shear sense and record south-side-up dip-slip shear.

Strain shadows occur locally in rocks of the Knife Lake Group and in the greenstone units of the Newton Lake Formation. During deformation, minerals are

locally displaced, rotated or rearrange by dilation and precipitation in dilation sites or sites of least stress. These sites can be strain shadows around rigid objects in the rock such as pyrite. Strain shadows form during low temperature metamorphism. Strain shadows within the Shagawa Lake shear zone are asymmetric and as such they make good shear sense indicators (Plate 2h). Sample 025 contains quartz strain shadows around pyrite. Strain shadows, commonly comprised of quartz, form around pyrite and opaque grain boundaries and result from growth of quartz grains along the instantaneous stretching axis. The long axis of the infinitesimal strain ellipse in plate 2h parallels the instantaneous stretching axis, which forms at an angle to foliation. The strain shadows in plate 2h indicate non-coaxial dextral shear parallel to strike-slip Le.

Extension fractures can also indicate shear sense. During non-coaxial shear fractures can open perpendicular to the instantaneous stretching direction. Within the fractures minerals precipitate and can grow in the direction of the instantaneous stretching axis giving a shear direction.

Calcite and quartz dominantly exist in fractures and veins and occasionally exhibit a grain-shape preferred orientation. Fractures with fibrous mineral fill are most common in the intermediate to mafic volcanic units of the Newton Lake Formation. The photomicrograph of sample 099-C is an example of a fibrous quartz-filled fracture within the greenstone of the Newton Lake Formation (Plate 2i). Quartz fibers are elongate parallel to maximum elongation, (or the maximum principal strain axis), and together with foliation and fracture orientations indicate a dextral shear sense as viewed in the photomicrograph.

Two samples record overprinting shear events. Sample 135 and 138 each contain microstructural evidence for south-side-up and north-side-up dip-slip shear (Plate 2j-k).

Sample 135, a fine-grained gray schist, contains white mica, plagioclase, calcite, chlorite, pyrite and quartz (Fig. 10). The protolith is possibly a felsic volcanic rock. S-planes are closely-spaced and transected by spaced C-planes, creating an S-C fabric. S-planes are defined by the preferred grain shape orientation of plagioclase and quartz. C-planes are defined by calcite and white mica. Together the S- and C-planes create an S-C fabric. Two distinct S-C fabrics are present in Sample 135. The dominant and pervasive fabric herein called $S_1$-$C_{1,}$ shows dextral shear sense and is best preserved in the upper and lower parts of the photomicrograph. A younger fabric, $S_2$-$C_2$, confined to a calcite-rich vein, records sinistral shear sense. The $S_2$-$C_2$ fabric within the calcite vein cross-cuts the more pervasively developed $S_1$-$C_1$ fabric. Therefore, $S_1$-$C_1$ fabric formed before the $S_2$-$C_2$ fabric that crosscuts it. Fabric $S_1$-$C_1$ indicates south-side-up shear parallel to dip-slip Le, and the $S_2$-$C_2$ fabric indicates north-side-up shear parallel to dip-slip Le. North-side-up shear is also less penetratively developed, and as such likely occurred at lower ductility then south-side-up shear. Lower ductility could result from lower temperature shear, higher strain rate, or an increase in sample strength due to earlier south-side-up shear.

Sample 138 indicates a similar kinematic history to that recorded in sample 135 (Fig. 11). Sample 138 is a fine-grained greenstone to greenschist metamorphic rock. Minerals include plagioclase, chlorite, quartz, white mica, siderite, opaque, and oxides. Chlorite is the main metamorphic mineral. The protolith might have been a felsic to mafic volcanic rock. Sample 138 displays two S-C-C' fabrics at different orientations.

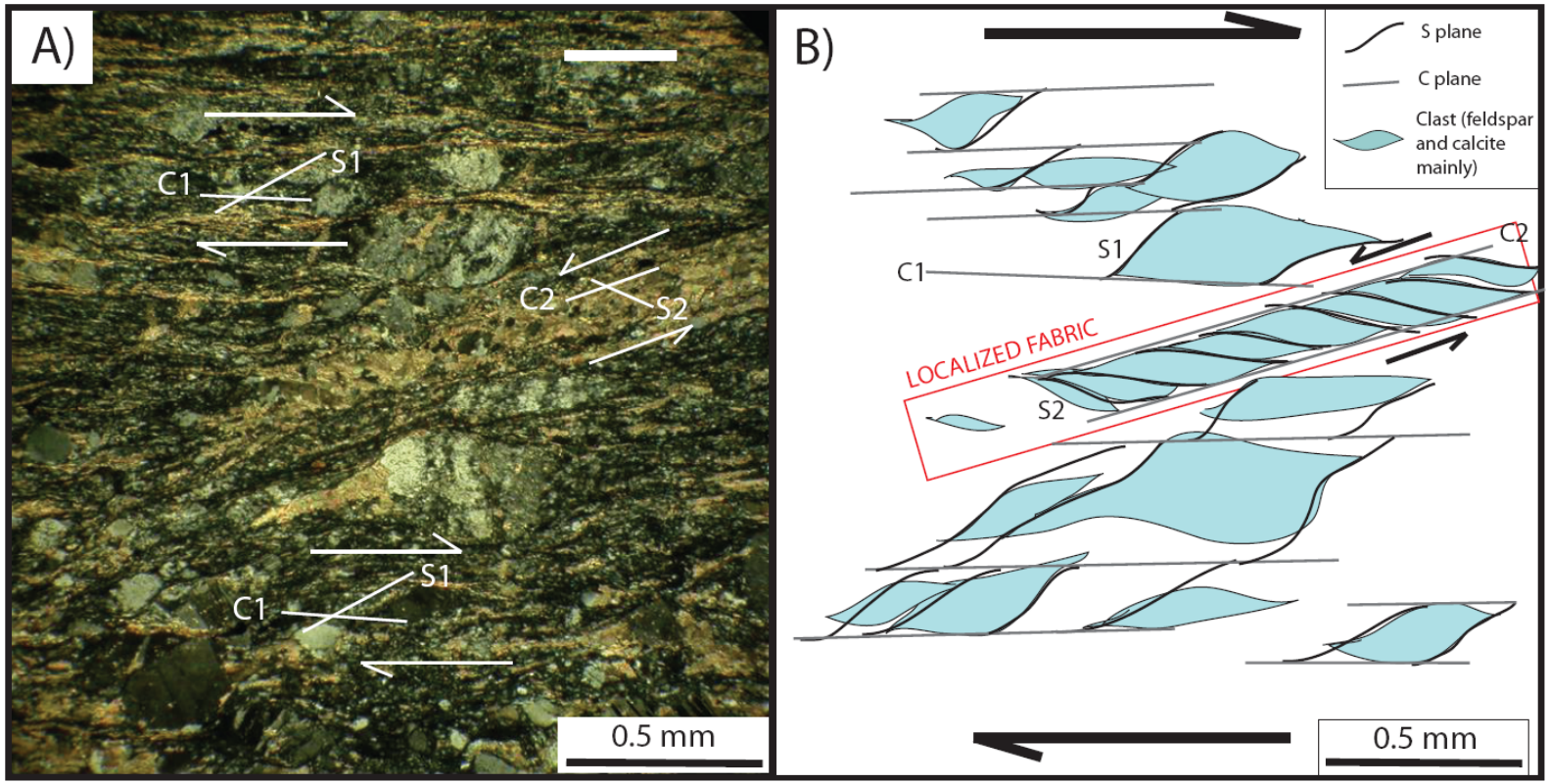


Figure 10. A) Photomicrograph of oriented sample 135 cut parallel to Le (motion plane) showing one pervasive S1-C1 fabric that displays dextral shear sense and one local S2-C2 fabric within a calcite vein that displays sinistral shear sense; thick line denotes the foliation strike; cross nicols. B) Sketch of photomicrograph A) showing S and C planes and clasts.

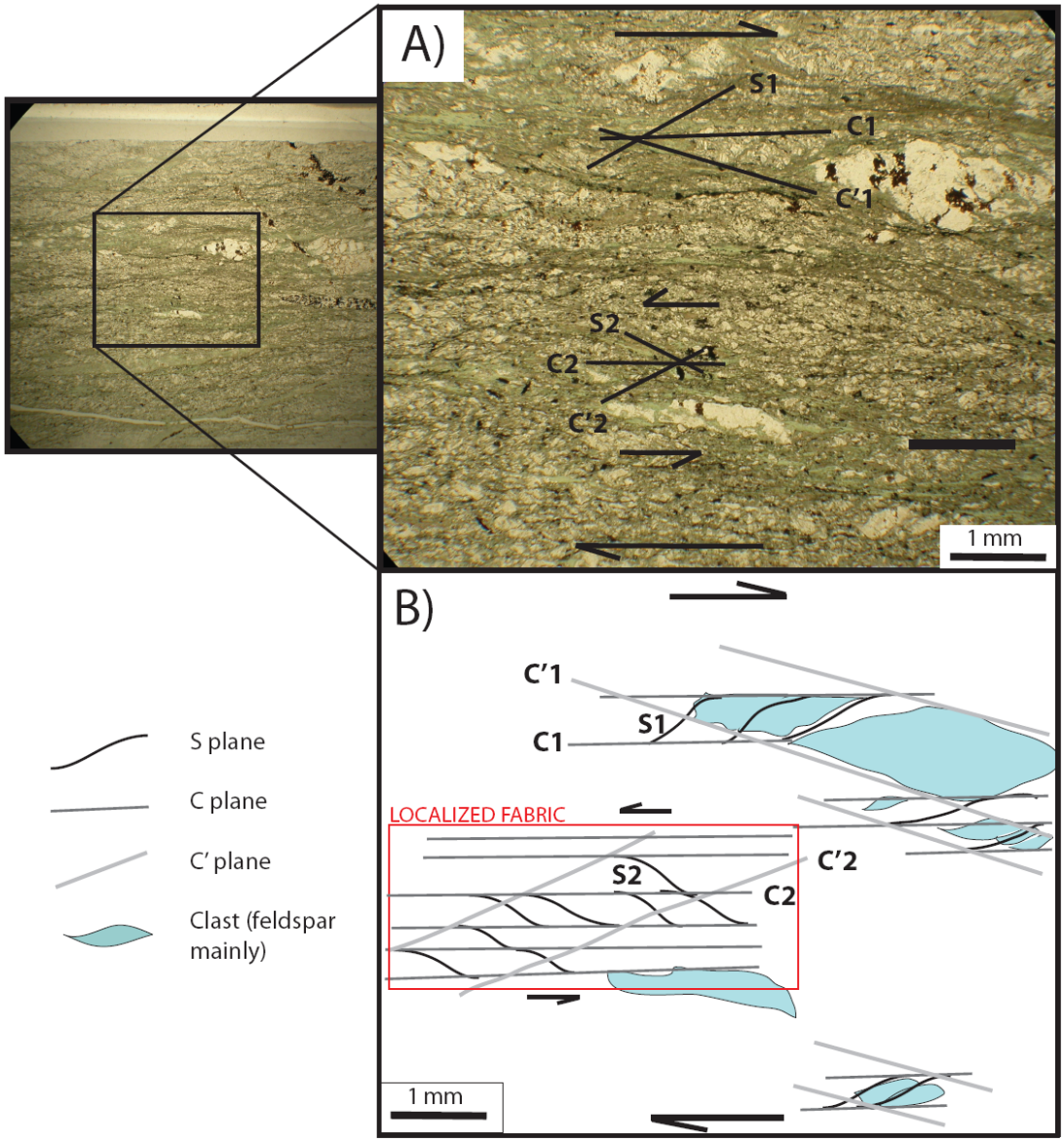


Figure 11. A) Photomicrograph of oriented sample 138 cut parallel to Le (motion plane) showing one pervasive S1-C1-C'1 fabric that displays dextral shear sense and one local S2-C2-C'2 fabric that displays sinistral shear sense; thick line at bottom right of photo denotes the foliation strike; plain polarized light. B) Sketch of photomicrograph A) showing S1-C1-C'1 and S2-C2-C'2 fabrics.

The alignment of chlorite and plagioclase define the S foliation. The alignment of chlorite defines the C foliation. The alignment of chlorite also defines C' planes. The C plane is consistently horizontal throughout the section. The dominant fabric $S_1$-$C_1$-$C'_1$ is penetratively developed throughout most of the thin section as preserved in the upper portion of the photomicrograph (Fig. 11). The dominant $S_1$-$C_1$-$C'_1$ fabric indicates dextral shear sense. The less penetratively developed fabric $S_2$-$C_2$-$C'_2$, (bottom of photomicrograph), is confined to a narrow zone within the thin section, and indicates sinistral shear sense. The $S_2$-$C_2$-$C'_2$ fabric domain appears to cross-cut the $S_1$-$C_1$-$C'_1$ fabric therefore the $S_2$-$C_2$-$C'_2$ fabric post-dates the $S_1$-$C_1$-$C'_1$ fabric. The $S_1$-$C_1$-$C'_1$ fabric records south-side-up shear parallel to dip-slip Le whereas, $S_2$-$C_2$-$C'_2$ fabric records north-side-up shear parallel to dip-slip Le. Sample 138, similar to sample 135, also shows that north-side-up shear is less penetratively developed and could also have resulted from lower ductility, higher strain rate, or increased sample strength from earlier south-side up shear.

Samples 135 and 138 each contain microstructural evidence for south-side-up and north-side-up dip-slip shear. Within each sample the two different shear senses occur within the same motion plane, which is parallel to Le and normal to foliation.

*Kinematic data*

Kinematic data from microstructural analysis is displayed on plate 3 along with foliation trajectories and Le orientation. Each small stereonet represents a thin section location and interpreted kinematic data. The stereonets display the kinematic data in the context of the local foliation and Le. Gray stereonets illustrate south-side-up shear sense and blue stereonets display north-side-up shear sense. Yellow stereonets illustrate

sinistral shear sense. Within the Le symbols on each stereonet the black half indicates which side moves downward (relative displacement). For samples with shallowly-plunging Le, shear sense is displayed in reference to the horizontal plane (sinistral) and with respect to Le. For samples with two shear events, the younger shear is indicated with a D (down) and U (up) within the stereonet. The kinematic confidence of each thin section location is shown with 5 (high) to 1 (low). Sample numbers are included within the stereonets.

Plate 3 illustrates some key kinematic spatial relationships. South-side-up and north-side-up shear both occur throughout the shear zone; no particular spatial pattern has been recognized. L-S tectonites with steeply-plunging Le occur throughout the shear zone. West- and east-plunging Le do not appear to occur in a distinct pattern. In the western part of the study area, a few L-S tectonites with north-side-up and south-side-up dip-slip shear occur. In the western part of the study area north-side-up shear is more centrally located with south-side-up shear occurring to the north and south. The study area becomes narrower to the east and L-S tectonites with south-side-up and north-side-up dip-slip shear appear randomly distributed from west to east and north to south. South-side-up and north-side-up dip-slip shear occur in close spatial proximity at some locations, such as those for samples 076, 010, 099-C and 106. Some L-S tectonites occur in the center of the shear zone at the west and east end of Fall Lake and at the west end of Shagawa Lake within the shear zone. Samples 135 and 138 both record south-side-up and north-side-up dip-slip shear and are in close spatial proximity. Therefore, *at the very least,* at the location of samples 135 and 138 south-side-up shear precedes north-side-up

shear. North-side-up shear could have post-dated south-side-up shear in other areas of the shear zone but no evidence was found in this study.

Evidence for strike-slip shear is limited to two sections within the shear zone. Four sections were cut parallel to strike-slip Le (Le pitch $0^{o}$-$30^{o}$). Strike-slip shear is only recorded within two sections and, in each case, it is less penetratively developed than dip-slip shear. The two sections (025-2 and 043-S) both display asymmetry that records sinistral shear sense. Sinistral shear occurs within two L-S tectonites with a shallowly east-plunging Le and a shallowly west-plunging Le. No dextral shear sense is recorded in sections from this study. The sections that record sinistral strike-slip shear occur in localized areas at the west and east end of the study area and are not connected in a linear zone along the shear zone. In the field strike-slip Le are localized, disconnected and overprint the dominant dip-slip Le. If strike-slip shear did occur within the Shagawa Lake shear zone, structural and kinematic evidence from this study indicates that it might have been sinistral, less pervasive and probably younger than the dominant dip-slip shear.

Kinematic data illustrated in plate 3 are summarized in Table 3 and categorized based on Le pitch and interpreted shear sense. Of the 34 sections that displayed shear sense asymmetric fabric, 32 yielded dip-slip shear sense and two yielded strike-slip shear sense indicators. Dip-slip shear sense indicators range in relative kinematic confidence from 1 (low) to 5 (high), with two 1's and one 5. The strike-slip shear sense indicators have a relative kinematic confidence of 4 and 3. The relative kinematic confidence for all sections averages 2 to 3. Only five sections have a kinematic confidence of 4 or 5. 16

# Table 3. Kinematic Summary

| Pitch (° from E) | Samples with interpreted shear sense | South up | North up | Dextral | Sinistral | Kinematic Confidence | | | | |
|---|---|---|---|---|---|---|---|---|---|---|
| | | | | | | 1 | 2 | 3 | 4 | 5 |
| 0-35 and 180-145 | 2 | 0 | 0 | 0 | 2 | 0 | 0 | 1 | 1 | 0 |
| 36-60 | 7 | 3 | 4 | 0 | 0 | 0 | 3 | 3 | 0 | 1 |
| 60-120 | 21 | 12 | 9 | 0 | 0 | 1 | 3 | 11 | 4 | 0 |
| 120-145 | 4 | 1 | 3 | 0 | 0 | 1 | 0 | 3 | 0 | 0 |
| Total | 34 | 16 | 16 | 0 | 2 | 2 | 6 | 18 | 5 | 1 |

sections record south-side-up dip-slip shear, 16 record north-side-up dip-slip shear and two record sinistral strike-slip shear. Of the seven sections that contained dip-slip Le pitch plunging to the east (36-60), three record south-side-up and four record north-side-up shear sense. Of the 21 sections that contained steeply-plunging dip-slip Le pitch (60-120) 12 record south-side-up shear sense. Of the sections that contained dip-slip Le pitch plunging to the west (120-145), the majority (3 of 4) record north-side-up shear sense.

Overall, L-S tectonites contain the following kinematic patterns: 1) Le pitch 60-120 record either south-side-up or north-side-up dip-slip shear; 2) Le pitch 35-60 record either south-side-up or north-side-up dip-slip shear; 3) Le pitch 120-145 dominantly indicate north-side-up shear and in addition, 4) shallow Le pitch (0-35 and 180-145) records sinistral shear; 5) north-side-up dip-slip shear overprints and is therefore younger than, south-side-up dip-slip shear, within two sections. Structural and kinematic data from this study indicates that oblique- to dip-slip shear was the most prominent deformation event in the Shagawa Lake shear zone.

### 4.3 Deformational History

Structural and kinematic data are consistent with two to three phases or events of deformation: 1) south-side-up oblique- to dip-slip shear, 2) north-side-up oblique- to dip-slip shear and, possibly 3) limited evidence for local sinistral strike-slip shear. The block diagrams in figure 12 illustrate structural and kinematic data projected through a slice of crust in the Shagawa Lake shear zone. The thick lines illustrate the relative location of shear based on kinematic shear sense indicators. The letters U and D illustrate relative up

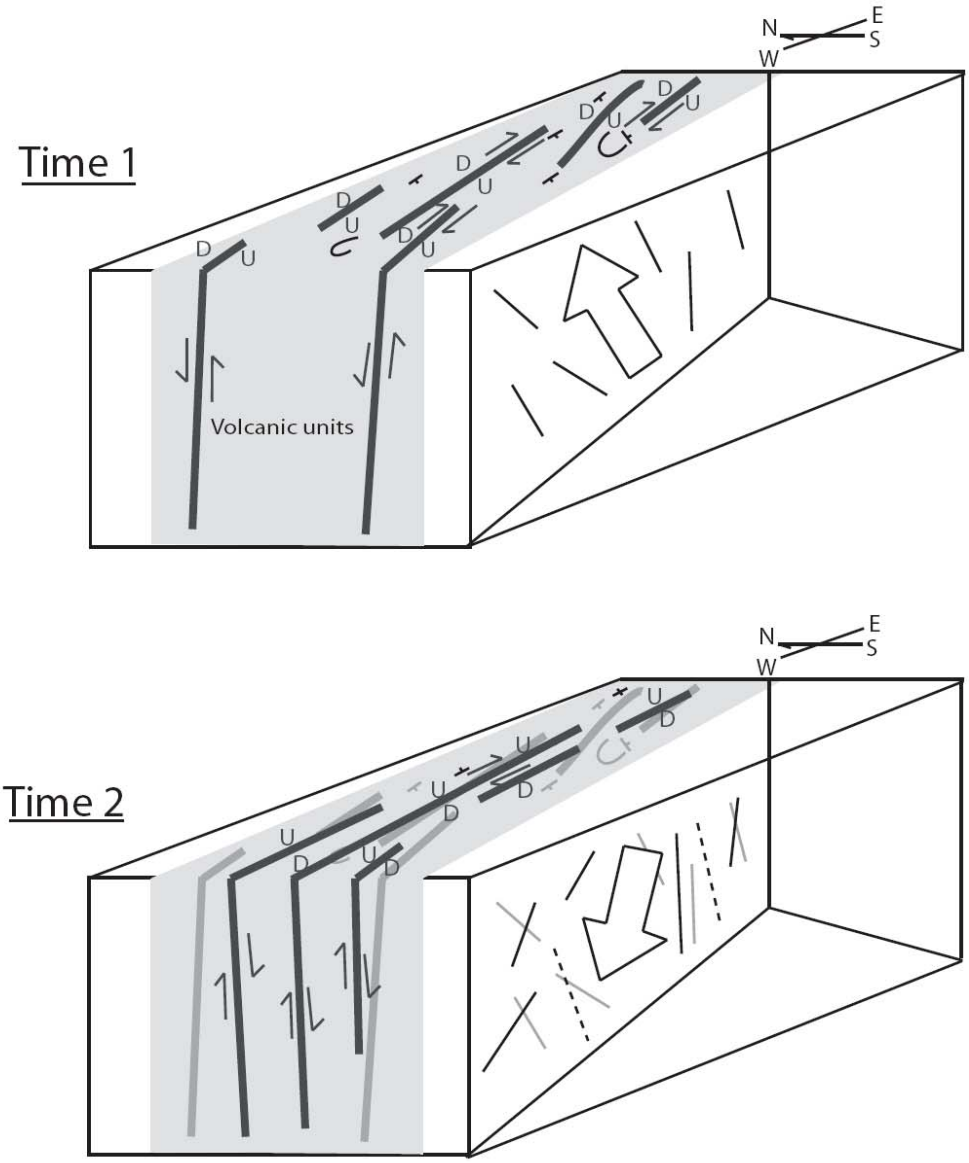


Figure 12. Cartoon block diagrams illustrating deformation events at time 1: south-side up dip-slip shear, Time 2: north-side up dip-slip shear. Thick arrows are movement directions and thin and dashed lines illustrate Le. Dashed Le in time 2 represent the east plunging Le that display north-side-up dip-slip shear. The location of the Shagawa Lake shear zone is outlined in gray.

and down shear, respectively. Apparent displacement directions are shown with arrows on the horizontal plane.

The first possible shear event was south-side-up parallel to dip-slip and oblique-slip Le (Fig. 12). South-side-up shear is overprinted locally by north-side-up shear. Samples 135 and 138 provide the only evidence for the relative timing of south-side-up versus north-side-up dip-slip deformation. Dip-slip L-S tectonites with east-plunging Le dominantly record south-side-up shear, whereas dip-slip L-S tectonites with west-plunging Le record north-side-up shear. Also, based on kinematic data, north-side-up shear is consistent with west-plunging Le.

The average orientation of the shear zone is east-northeast striking and steeply-dipping. Bedding planes become tilted during dip-slip shear and dip steeply to the south and north due to the formation of the steeply-dipping foliations within the shear zone. Minor folds could occur in the volcanic units as previously mapped in the shear zone (Sims and Mudrey, 1987).

Overall, the Shagawa Lake shear zone has experienced two dip-slip deformation events, south-side-up followed by north-side-up dip-slip shear. Evidence for strike-slip shear is limited to two samples. Sinistral strike-slip shear within the two samples is localized and not connected along the shear zone. It is clear, from this structural and kinematic analysis, that the Shagawa Lake shear zone experienced a complex deformational history.

## 5. Comparison with Previous Studies

Various structural and kinematic studies were performed within the Vermilion District and Shagawa Lake shear zone. Structural and kinematic data from this study is consistent with most past studies.

### 5.1 Dextral Transpression

Arc-terrane accretion involving transpression is invoked to explain the deformation of northeastern Minnesota (Bauer and Bidwell, 1990; Tabor and Hudleston, 1991; Jirsa et al., 1992; and Hudleston, 2003; Czech and Hudleston, 2004). Transpression, first termed to describe oblique convergence accommodated by folds and faults (Harland, 1971), today has many definitions and sub-classes. However, most importantly, transpression could be characteristic of both arc-terrane accretion and sagduction/diapirism processes. Thus, transpression should be used with caution in favoring models of granite-greenstone terrains formation.

The kinematic and structural study herein reveals why dextral transpression has historically been interpreted within the Shagawa Lake shear zone. It appears that previous workers considered displacement in the horizontal (geographic) plane, which is not the motion plane for oblique- to dip-slip shear within the shear zone (Bauer and Bidwell, 1990; Wolf, 2006; Hudleston et al., 1988). Kinematic data indicates five prevailing dip-slip shearing scenarios within the shear zone (Fig. 13). Blocks A and B display south-side-up dip-slip shear and blocks C, D and E display north-side-up dip-slip shear. Each scenario is referenced to plate 3 with a small stereonet that represents the shear sense and structural orientation of the block and also shows the apparent movement direction in the horizontal plane. Slices through blocks B, D and E illustrate the motion

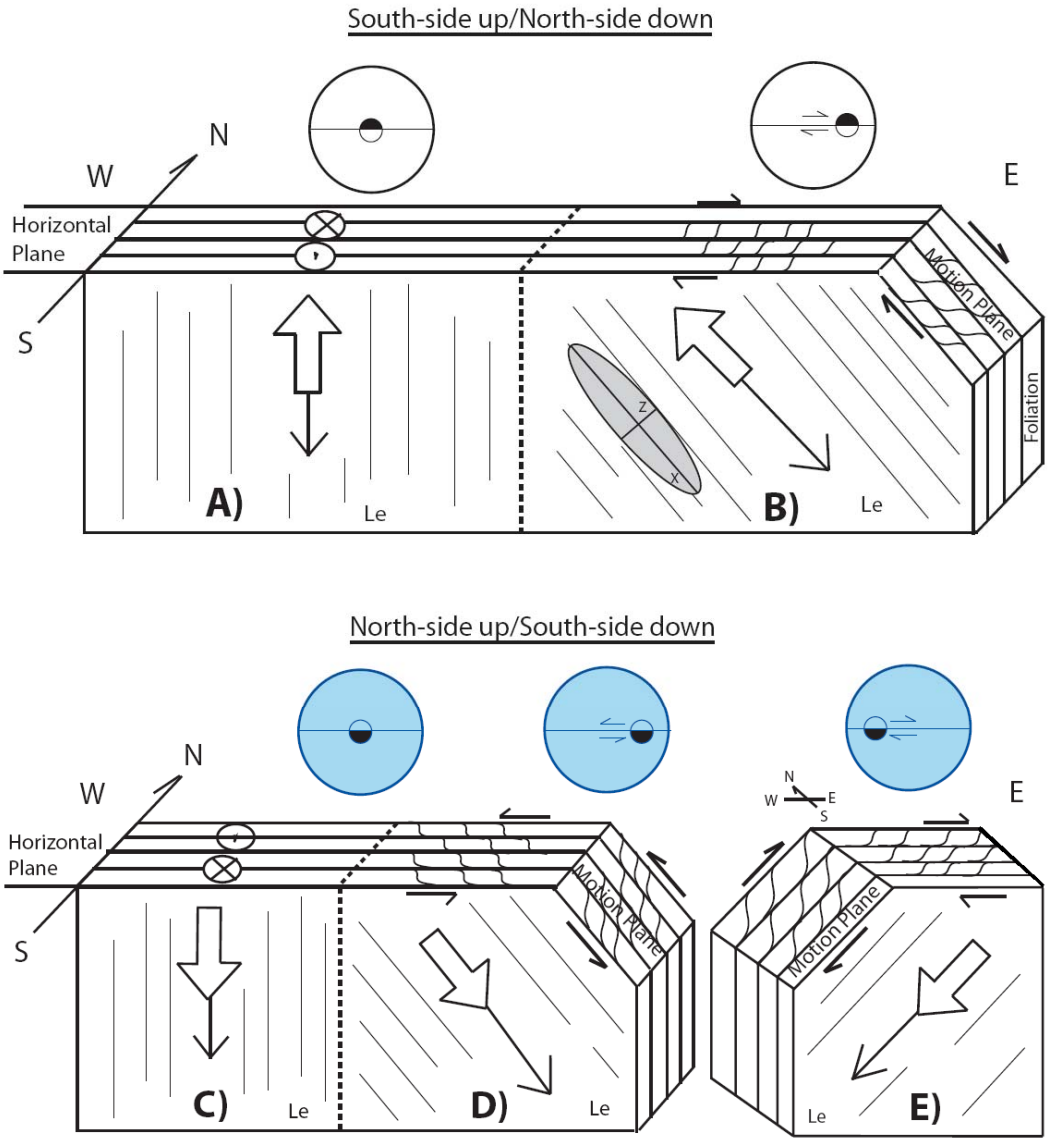


Figure 13. Block diagrams illustrating the relationship between shear sense (hollow arrows) and Le (thin lines) within Shagawa Lake shear zone L-S tectonites. A and C represent steeply-plunging Le showing south-side up and north-side up shear, respectively. B and E have obliquely-plunging Le, and show south-side up and north-side up, respectively. Both are more dominant than D. Le form parallel to maximum stretching direction X, shown in the strain ellipse. The stereonets represent the general kinematic orientation and apparent displacement in the horizontal plane for each block diagram as illustrated in Plate 3.

plane. Blocks A and C illustrate steeply-plunging Le that represent either south- or north-side-up dip-slip shear. East-plunging Le either record south-side-up dip-slip shear (Fig. 13 B) or north-side-up dip-slip shear (Fig. 13D). West-plunging Le dominantly record north-side-up, dip-slip shear (Fig. 13 E). Disregarding my samples with kinematic confidence of 1, six of 11 sections represent scenarios B and E. B and E both display *apparent* dextral shear sense in the horizontal plane. Data from this study indicate that the motion plane is not horizontal but rather, it is parallel to Le and as such generally steeply dipping. Dextral shear sense viewed in the horizontal plane is only *apparent.* The main deformation event is dip-slip shear. Transpression requires slip to occur along vertical and horizontal components. However, the deformation history herein infers that shear associated with the moderately- to steeply-plunging Le has a vertical or dip-slip component.

### 5.2 Bauer and Bidwell, (1990)

Bauer and Bidwell (1990) performed a structural and kinematic analysis of the Shagawa Lake shear zone mainly along the shoreline of Shagawa Lake and road outcrops (Fig. 6). A so-called C foliation strikes east-northeast and is steeply dipping to the south (Fig. 14A). Structural data indicate that Le plunges dominantly to the west and lies within the C foliation (Fig. 14B). The motion plane is parallel to Le and normal to foliation; Le formed parallel to the transport direction. All kinematic data reported by Bauer and Bidwell indicate dextral shear sense. The structural and kinematic data is illustrated in figure 14 showing the C foliation, dominant west-plunging Le and

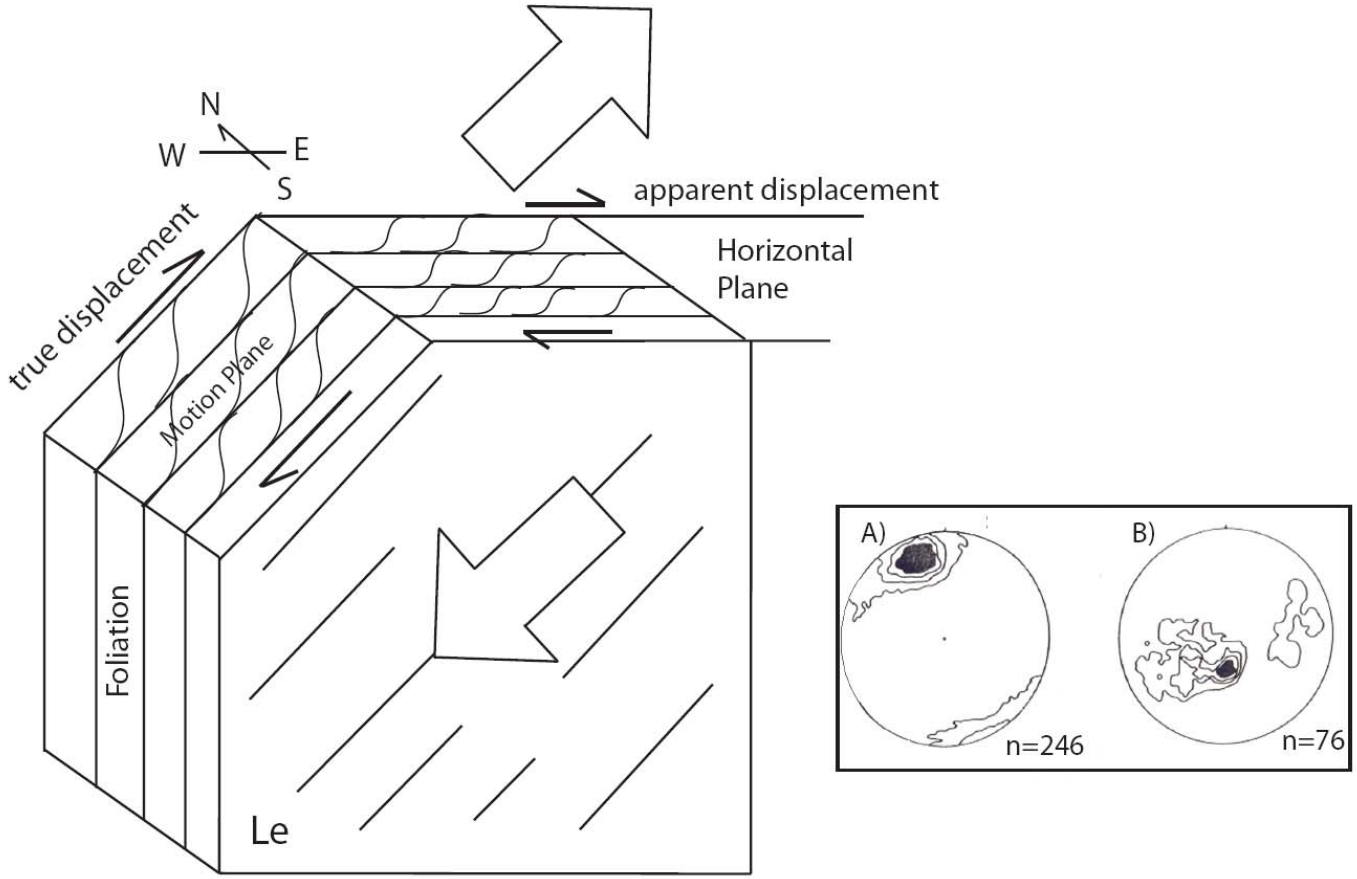


Figure 14. Block diagram of kinematic relationship interpreted for the Shagawa Lake shear zone by Bauer 1990. The lineation formed parallel to the transport direction. Thick arrows represent northwest-directed subduction; top is to the SE (lower plate to south subducts under the upper plate to the north ; see figure 16 for map). Apparent dextral displacement is shown in the horiztonal plane. Stereonets A and B show poles to C-foliation (contoured at 1, 5, 9, and 13%) and Le (contoured at 2, 6, 10, and 14%), respectively. (Data from Bauer and Bidwell, 1990).

consistent transport direction to the northwest. Bauer and Bidwell reported structural and kinematic data that indicate dextral transpression by way of northwest-directed subduction. A portion of the kinematic indicators and structural data herein represented by figure 13E and C are consistent with structural and kinematic data from Bauer and Bidwell's study.

### 5.3 Wolf (2006)

Wolf (2006) conducted a structural and kinematic study of the Shagawa Lake shear zone in Ontario, Canada. Wolf collected foliation and Le orientations from a ~10 km long and ~600 m wide zone of the Shagawa Lake shear zone. Metavolcanic and metasedimentary L-S tectonites contain an average orientation of 050, 75 NW. Le orientations are unclear. With 21 samples, oriented with respect to foliation, each were made into three mutually perpendicular thin sections and analyzed for microstructures. All microstructures found were consistent with sinistral shear sense. From structural and kinematic data Wolf interpreted that the Shagawa Lake shear zone underwent oblique sinistral thrusting where dip-slip and strike-slip displacement were accommodated simultaneously. Wolf's data are most consistent with data herein illustrated in the figure 13D and C block diagrams. The structural orientation and displacement of block diagram D is similar to Wolf's data. The horizontal plane in block diagram D only represents apparent sinistral displacement. Thus, Wolf's data is consistent with data herein represent in figure 13.

### 5.4 Hudleston et al. (1988)

Hudleston et al. (1988) performed a structural and kinematic analysis of the western Vermilion District. Foliation strikes E-W and dips steeply. Le plunges moderately to steeply to the east or west, parallel to the maximum stretching direction X (i.e. horizontal plane). Sigmoids and pressure shadows indicate a dextral strike-slip. Structural and kinematic data reported by Hudleston et al. (1988) are most consistent with data reported herein illustrating a east-striking steeply-dipping foliation with Le that plunge moderately to steeply to the east and west (Fig. 13A and B) and west (Fig. 13C and E). However, dextral strike-slip in the horizontal plane is not significant and only apparent for moderately- to steeply-plunging Le to the east and west.

Overall, structural and kinematic data herein encompass all three summarized previous studies. A portion of each data sets reported in this study in figure 13 can be correlated to data reported from Bauer and Bidwell (1990) (Fig. 13E and C), Wolf (2006) (Fig. 13D) and Hudleston et al. (1988) (Fig. 13A, B, C, E).

### 5.5 Bauer, (1985)

Bauer (1985) argued that deformation in the Vermilion District can be attributed to early recumbent folding ($F_1$) and younger upright folding ($F_2$) between the gneiss and greenstone boundary. $F_1$ folds are interpreted as early soft-sediment deformation and $F_2$ folds are defined as shear folds. Reported structural data includes: 1) $S_1$ parallels bedding, 2) $S_1$ is folded by $S_2$, 3) $F_2$ axial planes parallel $S_1$, and 4) both $S_1$ and $S_2$ are marked by micas. Questions arise as to what defines lineations and what is the difference between $S_1$ and $S_2$? A block diagram can best address these questions and was constructed from structural data reported by Bauer (1985).

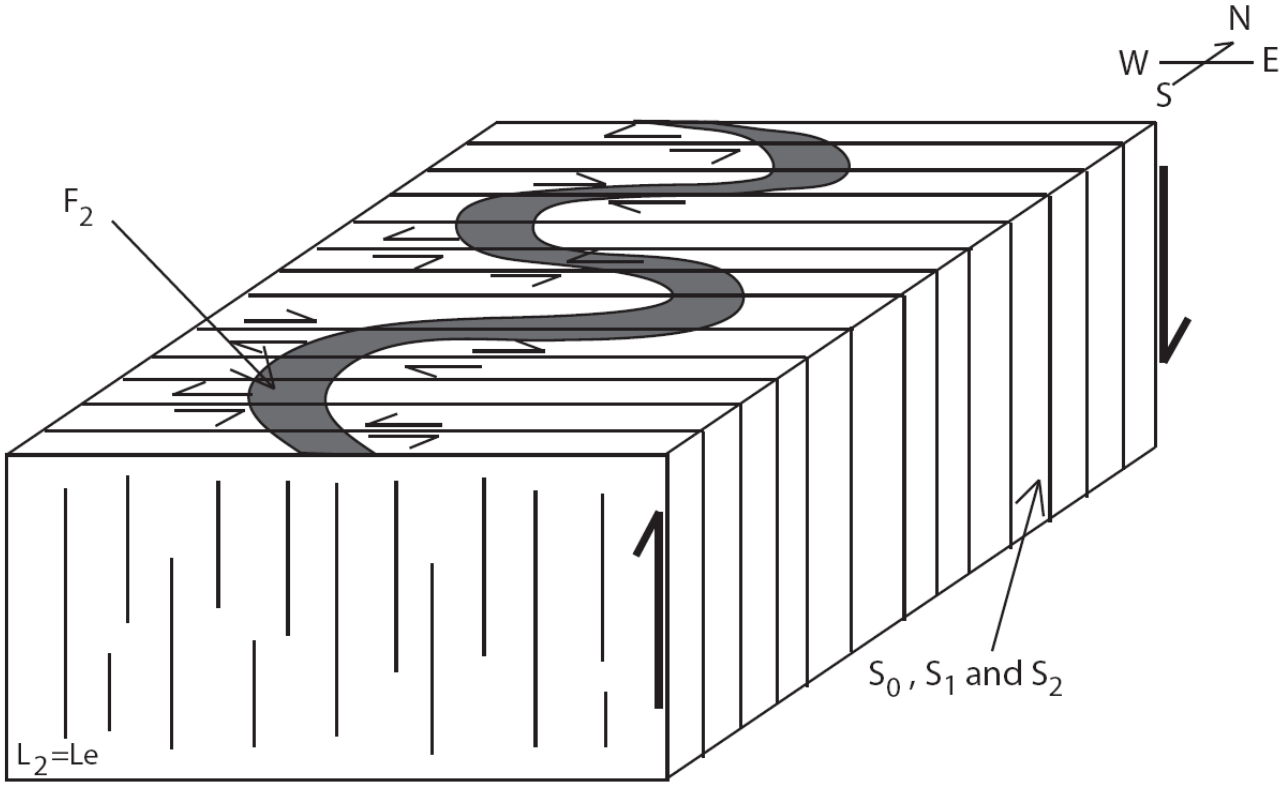


Figure 15. Block diagram of foliation, Le, and folds documented within the Vermilion District , northeastern Minnesota. $S_0$ (compositional layering), $S_1$ and $S_2$ are parallel and $L_2$ is a stretching lineation or elongation lineation (Le). $F_2$ fold axes parallel Le, and $F_2$ axial planes parallel $S_1$. (Data from Bauer, 1985)

A block diagram shows parallelism of compositional layering $S_0$, $S_1$, and $S_2$, $F_2$ axial planes parallel $S_1$, and $F_2$ fold axes parallel $L_2$ (Fig. 15). $L_2$, which lies within the foliation plane, is a mineral lineation. The $S_0$-$S_2$, $L_2$, $F_1$ and $F_2$ relationships outlined within previous work by Bauer (1985) (Fig. 15) are similar to the kinematic relationships in Sample 032 (Fig. 8). $F_1$ folds may have resulted from minor folding before the rocks were lithified. $F_2$ shear fold axes are parallel to $S_1$ and would take up small increments of deformation much like the kinematic relationship in Sample 032. The $F_2$ folding documented in Bauer's (1985) previous work is consistent with the relationship within sample 032 where incremental minor displacement occurs within the major dip-slip shear event. Thus, $F_2$ folding can be explained by mainly dip-slip shear and perpendicular small scale folding.

## 6. Evaluation of Hypotheses

Northwest-directed subduction with dextral transpression driven by arc-terrane accretion is the favored hypothesis based on previous studies within the Vermilion District and Shagawa Lake shear zone. The deformation history presented here favors sagduction/diapirism over arc-terrane accretion; however, this study reveals a more complex structural and kinematic history that might not be explained completely by only one hypothesis.

### 6.1 Arc-terrane Accretion

Previous studies have interpreted the Vermilion District and Shagawa Lake shear zone as a result of northwest-directed oblique subduction (Hudleston et al., 1988; Bauer and Bidwell, 1990). Figure 16 illustrates a map view of the structures that would occur within northwest-directed oblique subduction. Northwest-directed oblique subduction would predict: 1) through-going dextral strike-slip faults; 2) foliation strike would be linear, uniform and perpendicular to the convergence direction and; 3) only west-plunging Le that record north-side-up shear, *if* strain is *not* partitioned due to a high Archean geotherm. If strain is partitioned one would expect dip-slip shear with north-side-up displacement normal to the plate boundary, and concurrent dextral strike-slip parallel to the plate boundary.

Foliation trends within the Shagawa Lake shear zone are linear and roughly perpendicular to NW. However, Le orientations and kinematic data are not consistent with the predictions for arc-terrane accretion illustrated in figure 16. This study contains no evidence to support partitioned zones of dextral strike-slip displacement. Strike-slip

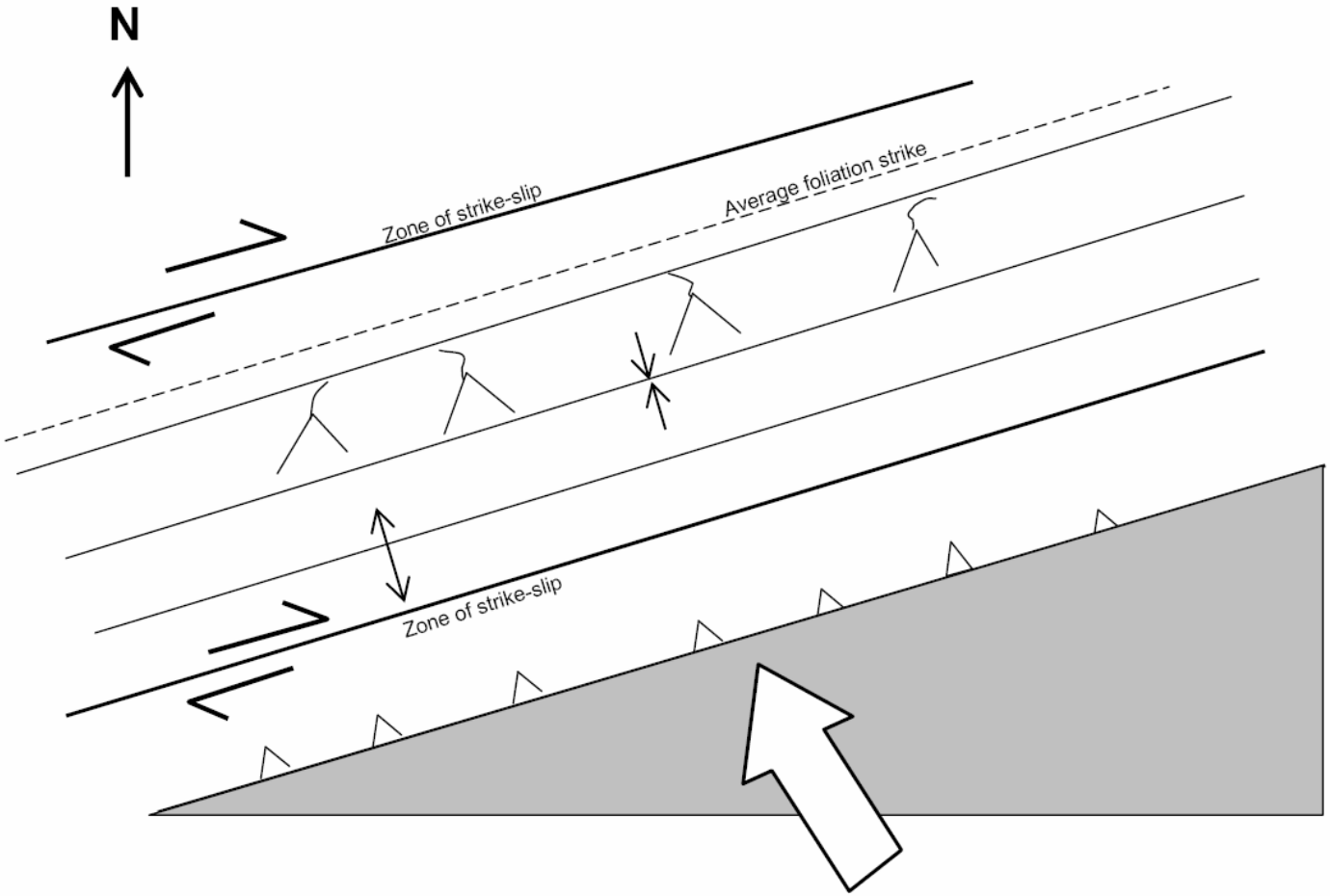


Figure 16. Cartoon map of northwest-directed subduction driven by arc-terrane accretion. Diagram represents an area that is larger than the Vermilion District and smaller than the Superior Province. Thick arrow represents subduction direction. Dashed line represents an average foliation strike.

evidence is limited to disconnected sinistral strike-slip in two locations within the shear zone. Also kinematic data reported herein are diverse. Dip-slip Le that plunges moderately to steeply to the east and west, records both south- and north-side-up displacement directions (Fig.13). It is challenging to resolve all the structural and kinematic data from this study with arc-terrane accretion.

*Folding*

South- and north-side-up dip-slip shear can not be explained by folding from subduction or convergence driven by arc-accretion. Figure 17 shows two models for folding. Time 1 in both models illustrates northward ductile movement and dextral shear sense with Le parallel to the transport direction. Model 1 applies recumbent folding that has a fold axis perpendicular to the movement direction. Recumbent folding in the orientation of model 1, time 2 would preserve the dextral shear sense within each limb of the fold. Model 1 is structurally consistent with the orientation and type of folding possible within a convergent geologic margin. However, model 1 does not create two opposing shear senses, and thus, cannot explain the occurrence of both south- and north-side-up dip-slip shear documented within the Shagawa Lake shear zone. Model 2 applies folding with a fold axis oriented parallel to the northward movement direction. In model 2, time 2 after folding, one limb would display dextral shear sense and the other would display sinistral shear sense. The folding illustrated in model 2, time 2 creates two opposing dip-slip shears (south- and north-side-up); one on each limb of the fold. However, fold axes parallel to the movement direction are not likely created by folding within the convergent setting illustrated in time 1. Overall, folding in any orientation within the convergent margin

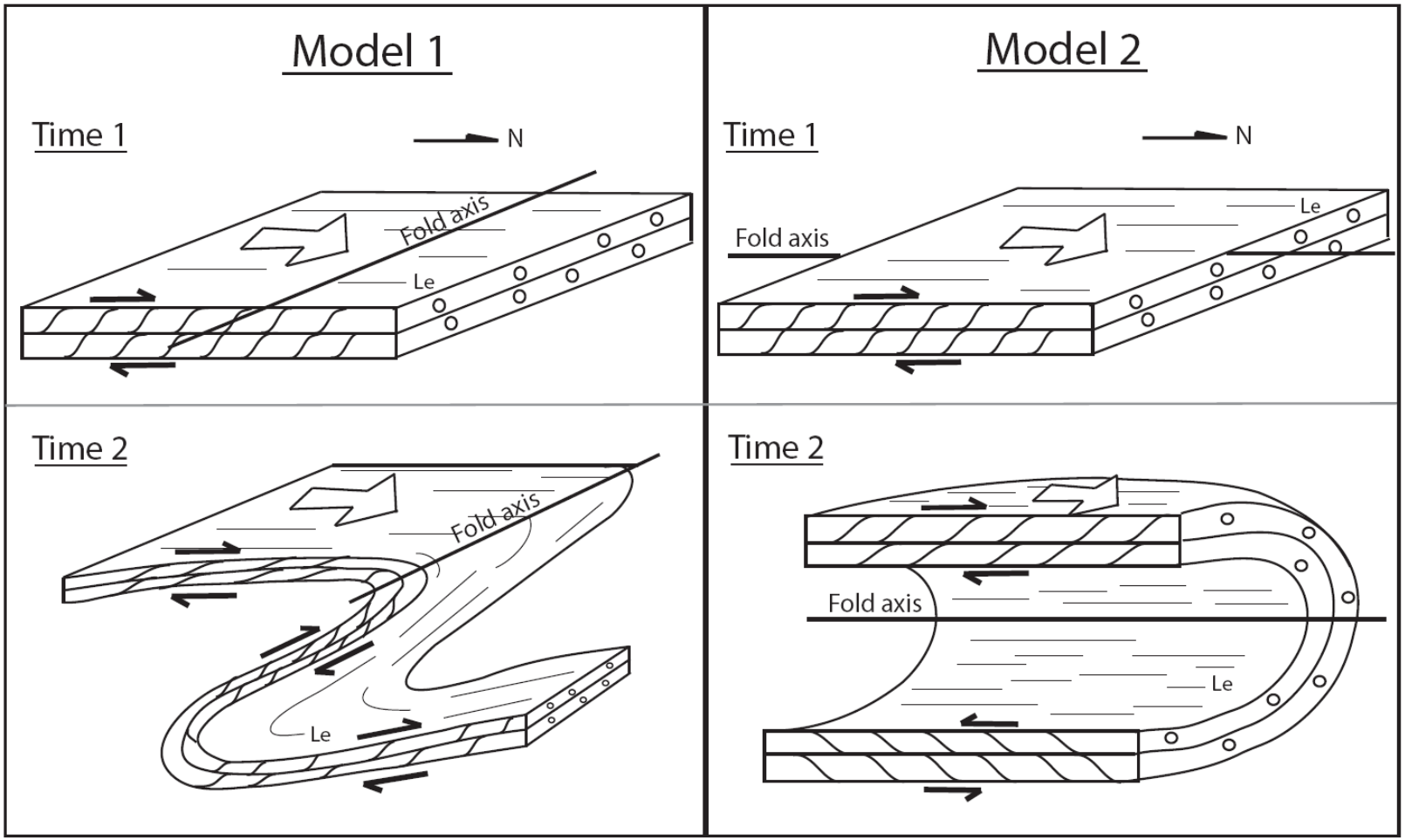


Figure 17. Diagrams illustrating two folding models with northward convergence. Each model shows the orientation of kinematic indicators. Le is represented as thin lines within each model. In Model 1, time 1, the fold axis is perpendicular to Le and kinematic indicators display dextral shear sense. In time 2, as folds form, dextral shear sense is perserved. Model 2, time 2 shows fold axes parallel to Le and dextral shear sense. As folds form in time 2, dextral and sinistral shear sense are displayed on opposite limbs of the fold. This type of folding is unlikely with the movement direction shown.

illustrated can not account for the occurrence of both south- and north-side-up dip-slip shear sense documented within the Shagawa Lake shear zone.

### 6.2 Sagduction/Diapirism

The history of the Shagawa Lake shear zone might be interpreted within the context of the sagduction/diapirism hypothesis. Dip-slip Le is dominant in the shear zone and is more easily reconciled with sagduction/diapirism (Fig. 18). The dominant east-plunging south-side-up dip-slip might be attributed to rise of the Giants Range Batholith. The consistent west-plunging north-side-up dip-slip shear might be attributed to rise of the Vermilion Granitic Complex. The overprinting kinematic indicators within samples 135 and 138 indicate that south-side-up shear pre-dated north-side-up shear at these locations. This relative time constraint could be accounted for with relative rise of the Giants Range Batholith followed by rise of the Vermilion Granitic Complex. Localized strike-slip could have formed during late stage deformation similar to but shallower than the deformation that formed the dip-slip Le. The rise of granitic complexes, to the south and north of the Shagawa Lake shear zone is currently the best way to accommodate the wide array of kinematic data reported in this study.

On the basis of sagduction/diapirism, one explanation for the lack of structural patterns is that the shear zone may have preferentially deformed across the entire shear zone during the rise of each granitic complex. The greater Archean lithospheric heat may have facilitated the dispersion of strain to extend across the entire shear zone. With the high geothermal gradient in the Archean, each episode of dip-slip shear (south and north-side up) in the L-S tectonites might be dispersed across the entire width of the shear

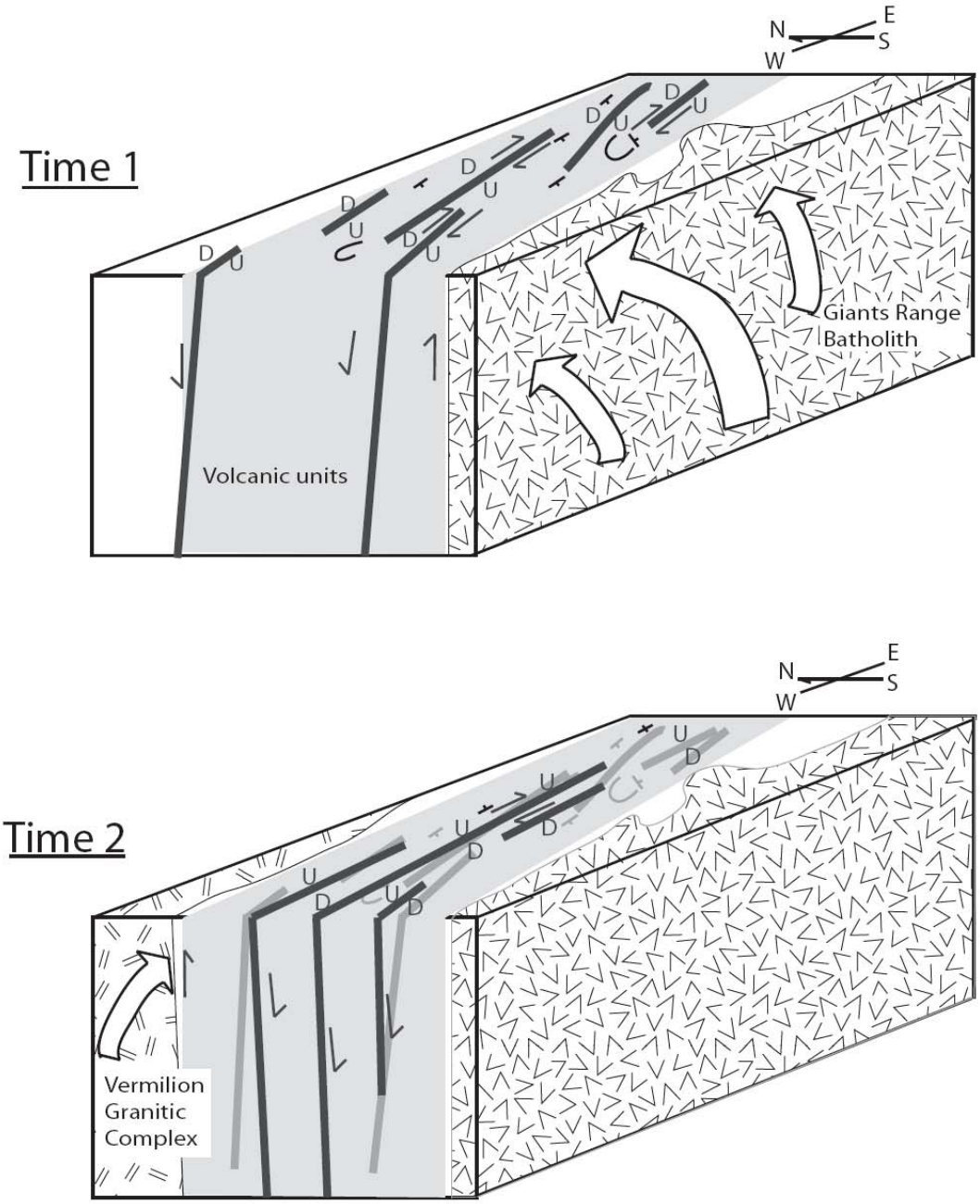


Figure 18. Cartoon block diagrams illustrating deformation events at Time 1: rise of the Giants range batholith resulting in south-side up dip-slip shear, Time 2: rise of the Vermilion Granitic Complex resulting in north-side up dip-slip shear. Gray area is the location of the Shagawa Lake shear zone.

zone. The associated north- and south-side up shear related to rise of granitic complexes would have no spatial pattern across or along the shear zone.

Further interpretation of structural and kinematic data indicates that the geologic time between the rise of the Giants Range Batholith and Vermilion Granitic Complex could have been relatively short or even temporarily at about the same time. East-plunging Le either display south-side-up or north-side-up shear sense. Kinematic evidence suggests that south-side-up shearing occurred before north-side-up shear. South-side-up shear is dominantly found within east-plunging Le and can be reconciled with rise of the Giants Range Batholith. How is east-plunging Le that record north-side-up shear explained? East-plunging Le that record north-side-up shear might result from rise of the Giants Range Batholith and Vermilion Granitic Complex at about the same geologic time. If both granitic complexes started to rise at the same time and in the same direction, then east-plunging Le would record both south-side-up and north-side-up shear. The Giants Range Batholith might cease rising before the Vermilion Granitic Complex which would account for the overprinting S-C fabrics within samples 135 and 138. Once the Giants Range Batholith stops rising and possibly influencing the rise of the Vermilion Granitic Complex, the Vermilion Granitic Complex might start to rise, resulting in west-plunging Le that record north-side-up shear. This sequence of rising granitic masses would explain the east-plunging Le that record both south-side-up and north-side-up shear. Hence, based on kinematic data presented herein, the Vermilion Granitic Complex may have risen just after the Giants Range Batholith.

Overall, sagduction/diapirism could account for the structural and kinematic pattern present in the Shagawa Lake shear zone. Sagging of greenstones and

simultaneous diapirism of the Giants Range Batholith followed by the Vermilion Granitic Complex granite could create steeply- to shallowly-plunging Le within volcanic and greenstone basins and account for the oblique- to dip-slip shear recorded in this study. Although the kinematic data reported herein appears consistent with the process of sagduction/diapirism other hypotheses cannot be excluded without further, more comprehensive studies of the granite-greenstone terrains in northeastern Minnesota.

## 7. Summary and Conclusions

The formation of Archean granite-greenstone terrains has been under debate, especially within the Superior Province. This structural and kinematic study of the Shagawa Lake shear zone sheds light on the debate within the Archean granite-greenstone terrains in northeastern Minnesota.

Structural and kinematic data within the Shagawa Lake shear zone highlights four relationships: 1) both south-side-up and north-side-up shear exist in no particular pattern along and across the shear zone, 2) east-plunging Le indicate both south- and north-side-up dip-slip shear, 3) west-plunging Le dominantly indicate north-side-up shear and, 4) limited evidence indicates that sinistral strike-slip shear occurred in localized zones that are not penetrative and overprint the early oblique- to dip-slip shear.

Microstructures in two L-S tectonites record south-side-up dip-slip shear that predated north-side-up dip-slip shear. The timing is consistent with early rise of the Giants Range Batholith followed by rise of the Vermilion Granitic Complex with concurrent sinking of greenstone basins in a process similar to sagduction/diapirism. The granites may become progressively shallower and transition from forming dip-slip Le to strike-slip Le but limited evidence for strike-slip shear halts further interpretation.

From this study, it is clear that the Shagawa Lake shear zone has a wonderfully complex deformational history that can be better understood from a more comprehensive study. Data from many shear zones in the same region can create a more complete structural and kinematic framework. Structural and kinematic data from the nearby Mud Creek, Burntside Lake, and Kawishiwi shear zones can supplement the data from the Shagawa Lake shear zone and provide additional insight into the Archean deformation

mechanisms within the Vermilion District (Karberg, 2008; Koester, 2008; Goodman, 2008).

## 8. References


Anhaeusser, C. R., Mason, R., Viljoen, M. J., and Viljoen, R. P., 1969. A reappraisal of some aspects of Precambrian Shield Geology. Geological Society of America Bulletin, 80, 2175-2200.

Arth, J. G. and Hanson, G. N., 1975. Geochemistry and origin of the early Precambrian crust of northeastern Minnesota. Geochimica et Cosmochimica Acta, 39, 325-362.

Bauer, R. L., 1985. Correlation of early recumbent and younger upright folding across the boundary between an Archean gneiss belt and greenstone terrane, northeastern Minnesota. Geology, 13, 657-660.

Bauer, R. L and Bidwell, M. E., 1990. Contrasts in the response to dextral transpression across the Quetico-Wawa subprovince boundary in northeastern Minnesota. Canadian Journal of Earth Sciences, 27, 1521-1535.

Bedard, J. H., Brouillette, P., Madore, L., and Berclaz, A., 2003. Archaean cratonization and deformation in the northern Superior Province, Canada: an evaluation of plate tectonics versus vertical tectonic models. Precambrian Research, 127, 61-87.

Bidwell, M., 1988. Structural analysis of shear zones in the central Vermilion District, NE Minnesota, Masters Thesis, University of Missouri.

Calvert, A. J., Sawyer, E. W., Davis, W. J., and J. N. Ludden, 1995. Archaean subduction inferred from seismic images of a mantle suture in the Superior Province. Nature, 375, 670-674.

Card, K. D., 1990. A review of the Superior Province of the Canadian Shield, a product of Archean accretion. Precambrian Research, 48, 99-156.

Cawood, P.A., 2006. Precambrian plate tectonics: Criteria and evidence. GSA Today, 16, 4-11.

Chadwick, B., Vasudev, V. N., and Hegde, G. V., 2000. The Dharwar craton, southern India, interpreted as the result of Late Archean oblique convergence. Precambrian Research, 99, 91-111.

Chardon, D., Peucat, J. J, Mudlappa, J., Choukroune, P., and Fanning, M. C., 2002. Archean granite-greenstone tectonics at Kolar (South India): Interplay of diapirism and bulk inhomogeneous contraction during juvenile magmatic accretion. Tectonics, 21, 1016-1033.

Collins, W. J., Van Kranendonk, M. J., and Teyssier, C., 1998. Partial convective overturn of Archaean crust in the east Pilbara Craton, Western Australia: driving mechanisms and tectonic implications. Journal of Structural Geology, 20, 1405-1424.

Condie, K. C., Allen, P., and Narayana, B. L., 1982. Geochemistry of the Archean Low- to High-Grade Transition Zone, Southern India. Contributions to Mineralogy and Petrology, 81, 157-167.

Czech, D. M., Hudleston, P. J., 2003. Testing models for obliquely plunging lineations in transpression: a natural example and theoretical discussion. Journal of Structural Geology. 25, 959-982.

Czeck, D. M. and Hudleston, P. J., 2004. Physical experiments of vertical tranpression with localized nonvertical extrusion. Journal of Structural Geology, 26, 573-581.

Engle, A. E. J., 1968. The Barberton Mountain Land: Clues to the differentiation of the Earth. Geological Society of South Africa, 71, 255-270.

Fowler, C. M. R., 2004, The Solid Earth: An Introduction to Global Geophysics Second Edition: Cambridge Press

Goodman, S., 2008. A Structural and Kinematic Analysis of the Kawishiwi Shear Zone, Superior Province: Insight on Granite-Greenstone Terrain Tectonics and Archean Crustal Evolution. Master's Thesis, University of Minnesota Duluth.

Green, J. C., 1970. Lower Precambrian Rocks of the Gabbro Lake Quadrangle, Northeastern Minnesota. Minnesota Geological Survey, Special Publication Series SP-13.

Green, J. C. and Schulz, K. J., 1982, Geologic map of the Ely quadrangle, St. Louis and Lake Counties, Minnesota. Minnesota Geological Survey, Miscellaneous Map Series M-50, scale 1:24000.

Green, J. C. Phinney, W. C. and Weiblen, P. W., 1966. Geologic Map of Gabbro Lake quadrangle, Lake County, Minnesota. Minnesota Geological Survey, Miscellaneous Map Series M-2, scale 1:31680.

Hanmar, S., Green, D. C., 2002. A modern structural regime in the Paleoarchean (~3.64) Isua Greenstone Belt, southern West Greenland. Tectonophysics, 346, 201-222.

Hanson, V. L., 1990. Collection and Preparation of thin sections of oriented samples. Journal of Geological Education, 38, 298.

Harland, W. B., 1971. Tectonic transpression in Caledonian Spitzbergen. Geological Magazine, 108, 27-47.

Hickman, A. H., 2003. Two contrasting granite-greenstone terranes in the Pilbara Craton, Australia: evidence for vertical and horizontal tectonic regimes prior to 2900 Ma. Precambrian Research, 131, 153-172.

Hooper, P.R., and Ojakangas, R. W., 1971. Multiple Deformation in Archean Rocks of the Vermilion District, Northeastern Minnesota. Canadian Journal of Earth Sciences, 8, 423-434.

Hudleston, P. J., Schutz-Ela, D., and Southwick, D. L., 1988. Transpression in an Archean greenstone belt, northern Minnestoa. Canadian Journal of Earth Sciences, 25, 1060-1068.

Jirsa, M. A., Miller, J. D., 2004. Bedrock Geology of the Ely and Basswood Lake 30' X 60' quadrangles, northeastern, Minnesota. Minnesota Geological Survey. Misc Map Series, M-148, scale 1:100000.

Jirsa, M. A., Southwick, D. L, and BoerBoom, T. J., 1992. Structural evolution of Archean rocks in the western Wawa subprovince, Minnesota: refolding of precleavage nappes during D2 transpression. Canadian Journal of Earth Science, 29, 2146-2155.

Karberg, S. M., 2008. Structural and Kinematic Analysis of the Mud Creek Shear Zone, northeastern Minnesota: Implications for Archean (2.7 Ga) Tectonics. Master's Thesis, University of Minnesota Duluth.

Kimura, G., Ludden, J. N., Desrochers, J.-P., and Hori, R., 1993. A model of ocean-crust accretion for the Superior Province, Canada. Lithos, 30, 337-355.

Koester, J., 2008. Structural, kinematic and Petrographic analysis of the Burntside Lake shear zone: Master's Thesis, University of Minnesota Duluth.

Krapez, B. and Barley, M. E., 2008. Late Archaean synorogenic basins of the Eastern Goldfields Superterrane, Yilgarn Craton, Western Australia Part III. Signatures of tectonic escape in an arc-continent collision zone.

Lambert, R. St J., 1980 The thermal history of the earth in the Archean. Precambrian Research, 11, 199-213.

Lin, S., 2005. Synchronous vertical and horizontal tectonism in the Neoarchean: Kinematic evidence from a synclinal keel in the northwestern Superior craton, Canada. Precambrian Research, 139, 181-194.

Mareschal, J.-C. and West. G. F., 1980. A model for Archean tectonism. Part 2. Numerical models of vertical tectonism in greenstone belts. Canadian Journal of Earth Science, 17, 60-71.

McGregor, A. M. 1951. Some milestones in the Precambrian of South Rhodesia. Parts 1-3. Transactions of the Geological Society of South Africa, 54, 27-71.

Morey, J. B., J, Meints, 2000. Geologic Map of Minnesota Bedrock Geology, Third Edition. Minnesota Geological Survey .State Map Series, S-20, scale 1:1000000.

Passchier, C.W., Trouw, R.A.J., 2005, Microtectonics Second Edition: Berlin, Heidelberg, Springer-Verlag Publishing.

Percival, J. A., and Williams, H. R., 1989. Late Archean Quetico accretionary complex, Superior Province, Canada. Geology, 17, 23-25.

Parmenter, A. C., Lin, S., Corkery, T. M., 2006. Structural evolution of the Cross Lake greenstone belt in the northwestern Superior Province, Manitoba: implications for relationships between vertical and horizontal tectonism. Candian Journal of Earth Science, 43, 767-787.

Rey, P. F. and Houseman, G., 2006. Lithospheric scale gravitational flow; the impact of body for orogenic processes from Archaean to Phanerozoic, in Buiter S. J. H., and Schreurs, G., eds., Analysis and numerical modeling of crustal-scale processes. London, Geological Society Special Publication, 253, 153-167.

Rey, P. F., Philippot, P., and Thebaud, N., 2003. Contributions of mantle plumes, crustal thickening and greenstone blanketing to the 2.75-2.65 Ga global crisis. Precambrian Research, 127, 43-60.

Sandiford, M., Van Kranendonk, M. J., and Bodorkos, S., 2004. Conductive incubation and the origin of the dome-and-keel structure in Archean granite-greenstone terrains: A model based on the eastern Pilbara Craton, Western Australia. Tectonics, 23.

Schulz, K. J., 1980. The magmatic evolution of the Vermilion Greenstone Belt, NE Minnesota. Precambrian Research, 11, 215-245.

Sims P. K., 1976. Early Precambrian tectonic-igneous evolution in the Vermilion district, northeastern Minnesota. US Geological Survey, 87, 379-389.

Sims, P. K. and Mudrey, M. G., 1978, Geologic map of the Shagawa Lake quadrangle, St. Louis County, Minnesota: U.S. Geological Survey, Geologic Quadrangle Map GQ-1423, scale 1:24000.

Stanley, S.M., 1992. *Earth System History*. W.H. Freeman and Co., New York.

Tabor, J. R., Hudleston, P. J., 1991. Deformation at an Archean subprovince boundary, northern Minnesota. Canadian Journal of Earth Science, 28, 292-307.

Tikoff, B. and Peterson K., 1998. Physical Experiments of transpressional folding. Journal of Structural Geology. 20, 661-672.

Van Kranendonk, M. J., Collins, W. J., Hickman, A., and Pawley, M. J., 2004. Critical tests of vertical vs. horizontal tectonic models for the Archaean East Pilbara Granite-Greenstone Terrane, Pilbara Craton, Western Australia. Precambrian Research, 131, 173-211.

West. G. F., and Mareschal, J.-C., 1979. A model of Archean tectonism; Part 1, The thermal conditions. Canadian Journal of Earth Sciences, 16, 1942-1950.

Windley, B. F., 1984. The evolving continents, 2nd Edition. Chichester-Wiley, London.

Winter, J. D., 2001. An Introduction to Igneous and Metamorphic Petrology. Prentice Hall.

Wolf, D. E., 2006. The Burntside Lake and Shagawa/Knife Lake shear zones: Deformation kinematics, geochemistry and geochronology; Wawa Subprovince, Ontario, Canada. Masters Thesis, Washington State University.

Zahnle, K. J., 2006. Earth's Earliest Atmosphere. Elements, 2, 217-222.